Modeling of Spatially-Dispersive Wire Media: Transport Representation, Comparison With Natural Materials, and Additional Boundary Conditions

George W. Hanson, *Fellow, IEEE*, Ebrahim Forati, *Student Member, IEEE*, and Mário G. Silveirinha, *Member, IEEE*

Abstract—**Natural and artificial wire materials exhibiting spatial dispersion are considered using a transport (drift-diffusion) model. The connection between drift-diffusion and electron transport in natural materials is highlighted, and then applied to various forms of wire media, leading to the definition of effective conductivity and diffusion parameters that characterize the material. It is shown that the effective material parameters lead to a Debye length that provides a quantitative measure of the strength of spatial dispersion for wire mediums. Further, it is shown that Pekar's additional boundary condition applies in many instances to natural materials as well as artificial wire media, and can be derived from elementary electromagnetics.**

Index Terms—**Diffusion, metamaterial, plasma, wire medium.**

I. INTRODUCTION

NATURAL optical activity, bianisotropy, and excitonic effects are associated with spatial dispersion (non-locality) in many natural solids [1]–[3], where the effect is often quite small far below the plasma frequency at room temperature, but may be important either at very low temperature (e.g., the anomalous skin effect [4]), or near the plasma frequency (e.g., ordinary metals [3] and excitonic semiconductors). Although many natural materials have plasma frequencies in the optical or ultra-violet, low-density plasmas and semiconductors, and many artificial materials such as wire media, have effective plasma frequencies in the GHz or THz range. Particularly because of the emerging importance of wire media for GHz through mid-THz applications, the concept of spatial dispersion has gained great importance in the engineering electromagnetics community, for both bulk and surface effects [5]–[14]. Furthermore, it has been shown that wire media may enable manipulating, transporting and measuring the near-field, subwavelength imaging, and complex operations such magnification and demagnification [9]–[12].

Preliminary investigation of the transport model for artificial materials was presented in [15]. The main ideas of this paper are 1) to further develop and discuss the transport/drift-diffusion model for several types of wire metamaterials, both isotropic and anisotropic, including a new double mesh form, 2) to compare the degree of spatial dispersion in natural and artificial materials using an effective Debye length as a quantitative measure, and 3) to discuss a fairly general additional boundary condition that is applicable to a wide class of natural and artificial materials. We present a simple one-dimensional example with closed-form solution that highlights these topics, and also present a new solution of transmission through a double wire mesh medium.

II. TRANSPORT MODEL OF NATURAL AND ARTIFICIAL MATERIALS

A. Natural Materials – Plasmas and Semiconductors

For natural materials the drift-diffusion equation arises from a series of approximations of basic transport processes. In the following we briefly review the main assumptions in deriving the drift-diffusion equation for natural materials, since this is helpful to interpret the range of validity of the formulation. Furthermore, this leads to the transform-domain permittivity (17) needed in the next section.

We assume semi-classical transport governed by the Boltzmann equation, such that for charge species α we can define a distribution function $f_\alpha(\mathbf{r}, \mathbf{v}, t)$ that satisfies Boltzmann's equation. Conservation of charge (continuity equation) and conservation of momentum (transport equation) are derived by taking moments of Boltzmann's equation [16, Ch. 8]. The first moment leads to the continuity equation

$$\frac{\partial \rho_\alpha(\mathbf{r}, t)}{\partial t} + \nabla \cdot \mathbf{J}_\alpha^{\text{cond}}(\mathbf{r}, t) = 0 \qquad (1)$$

where $\rho_\alpha(\mathbf{r}, t) = q_\alpha n_\alpha(\mathbf{r}, t)$ is the charge density, $n_\alpha(\mathbf{r}, t) = \int f_\alpha(\mathbf{r}, \mathbf{v}, t) d^3v$ is the number density, and $\mathbf{J}_\alpha^{\text{cond}}(\mathbf{r}, t) = q_\alpha n_\alpha(\mathbf{r}, t) \mathbf{v}_\alpha(\mathbf{r}, t) = q_\alpha \int \mathbf{v} f_\alpha(\mathbf{r}, \mathbf{v}, t) d^3v$ is the conduction current density ($\mathbf{v}_\alpha$ is average velocity).

The transport equation is obtained from the second moment of Boltzmann's equation [16],

$$\frac{\partial}{\partial t}\left(n_\alpha(\mathbf{r}, t) \mathbf{v}_\alpha(\mathbf{r}, t)\right) + \beta_\alpha \nabla n_\alpha(\mathbf{r}, t)$$
$$+ n_\alpha(\mathbf{r}, t)(\mathbf{v}_\alpha \cdot \nabla) \mathbf{v}_\alpha + \mathbf{v}_\alpha \nabla \cdot n_\alpha(\mathbf{r}, t) \mathbf{v}_\alpha$$
$$- \frac{q_\alpha}{m_\alpha} n_\alpha(\mathbf{r}, t) \mathbf{E}(\mathbf{r}, t) + \frac{1}{\tau_\alpha} n_\alpha(\mathbf{r}, t) \mathbf{v}_\alpha = 0 \qquad (2)$$

where $\beta_\alpha = \langle v_\alpha^2 \rangle /3$, with $\langle v_\alpha^2 \rangle$ being the mean-square velocity of the charge carrier. For plasmas $\langle v_{\alpha,\ \text{thermal}}^2 \rangle = 3 k_B T_\alpha / m_\alpha$ but for good metals $\langle v^2 \rangle = 3 v_F^2 /5$, where v_F is the electron Fermi velocity. In deriving (2) we have ignored gravity, and magnetic field effects in the Lorentz force (thus we assume no large magnetic bias field) compared to the much stronger electric force. Further, in obtaining (2) the kinetic pressure dyad $\overline{\mathbf{P}}_\alpha$ has been approximated as $p_\alpha \mathbf{1}$, where $p_\alpha = n_\alpha k_B T_\alpha$ is the scalar kinetic pressure [16, pp. 149–152, 202]; this approximation closes the system of equations, and corresponds to ignoring tangential shear/viscous forces (off-diagonal elements of $\overline{\mathbf{P}}_\alpha$) and assuming an isotropic particle velocity distribution. More generally, the term $k_B T_\alpha \nabla n_\alpha$ is expressed as $\nabla \cdot \overline{\mathbf{P}}_\alpha$. Finally, we have assumed that collisions are represented by a phenomenological relaxation time τ_α.

The transport equation is nonlinear, and the next step in deriving the drift-diffusion equation is to linearize the transport equation, writing

$$n_\alpha (\mathbf{r}, t) = N_\alpha + n_\alpha^s (\mathbf{r}, t) \quad (3)$$

where n_α^s is a small deviation from the equilibrium density N_α (i.e., when $\mathbf{E} = \mathbf{0}$, $n_\alpha (\mathbf{r}, t) = N_\alpha$, associated with the equilibrium Fermi distribution) induced by the small applied field $\mathbf{E}(\mathbf{r}, t)$. The resulting (drift) velocity $\mathbf{v}_\alpha (\mathbf{r}, t)$ is small, and the transport equation becomes, upon discarding second- and higher-order terms,

$$\left(\frac{\partial}{\partial t} + \frac{1}{\tau_\alpha} \right) \mathbf{J}_\alpha^{\text{cond}} (\mathbf{r}, t) + \beta_\alpha \nabla \rho_\alpha^s (\mathbf{r}, t) - \frac{q_\alpha^2}{m_\alpha} N_\alpha \mathbf{E}(\mathbf{r}, t) = 0 \quad (4)$$

where $\rho_\alpha^s (\mathbf{r}, t) = q_\alpha n_\alpha^s (\mathbf{r}, t)$ and the linearized current is

$$\mathbf{J}_\alpha^{\text{cond}} (\mathbf{r}, t) = q_\alpha N_\alpha \mathbf{v}_\alpha (\mathbf{r}, t) . \quad (5)$$

The charge density $q_\alpha N_\alpha$ is constant in space and time; it is only for this linearized form that a time-harmonic electric field will maintain a time-harmonic current $\mathbf{J}$ (via time-harmonic velocity $\mathbf{v}$), and time-harmonic excess number density n_α^s. Writing

$$\mathbf{J}_\alpha^{\text{cond}} (\mathbf{r}, t) = \mathbf{J}_\alpha^{\text{cond}} (\mathbf{r}) e^{j\omega t} \to \mathbf{v}_\alpha (\mathbf{r}, t) = \mathbf{v}_\alpha (\mathbf{r}) e^{j\omega t} \quad (6)$$

$$n_\alpha (\mathbf{r}, t) = N_\alpha + n_\alpha^s (\mathbf{r}, t) = N_\alpha + n_\alpha^s (\mathbf{r}) e^{j\omega t} \quad (7)$$

$$\mathbf{E}(\mathbf{r}, t) = \mathbf{E}(\mathbf{r}) e^{j\omega t}, \quad (8)$$

we have, using $\rho_\alpha^s (\mathbf{r}) = q_\alpha n_\alpha^s (\mathbf{r})$, the drift-diffusion equation

$$\mathbf{J}_\alpha^{\text{cond}} (\mathbf{r}, \omega) = \sigma_\alpha (\omega) \mathbf{E}(\mathbf{r}, \omega) - D_\alpha (\omega) \nabla \rho_\alpha^s (\mathbf{r}, \omega) \quad (9)$$

$$= \mathbf{J}^{\text{cond,local}} + \mathbf{J}^{\text{cond,nonlocal}} \quad (10)$$

where

$$\sigma_\alpha = \frac{q_\alpha^2 \tau_\alpha N_\alpha}{m_\alpha (1 + j\omega \tau_\alpha)}, \quad D_\alpha = \frac{\beta_\alpha \tau_\alpha}{(1 + j\omega \tau_\alpha)}. \quad (11)$$

The term associated with diffusion is clearly nonlocal, since the gradient samples the charge in a neighborhood of $\mathbf{r}$.

The linearized continuity equation is

$$j\omega \rho_\alpha^s (\mathbf{r}) + \nabla \cdot \mathbf{J}_\alpha^{\text{cond}} (\mathbf{r}, t) = 0 \quad (12)$$

and therefore the drift-diffusion equation becomes

$$\left(\mathbf{1} - \frac{D_\alpha (\omega)}{j\omega} \nabla \nabla \right) \cdot \mathbf{J}_\alpha^{\text{cond}} (\mathbf{r}, \omega) = \sigma (\omega) \mathbf{E}(\mathbf{r}, \omega) \quad (13)$$

($\mathbf{1}$ is the identity dyadic) such that

$$\mathbf{J}_\alpha^{\text{cond}} (\mathbf{r}, \omega) = \sigma (\omega) \left(\mathbf{1} - \frac{D_\alpha (\omega)}{j\omega} \nabla \nabla \right)^{-1} \cdot \mathbf{E}(\mathbf{r}, \omega) . \quad (14)$$

Transformation into the spatial transform plane ($\mathbf{q} \leftrightarrow \mathbf{r}$) leads to $\mathbf{J}_\alpha^{\text{cond}} (\mathbf{q}, \omega) = \overline{\boldsymbol{\sigma}}_\alpha (\mathbf{q}, \omega) \cdot \mathbf{E}(\mathbf{q}, \omega)$, where [15]

$$\overline{\boldsymbol{\sigma}}_\alpha (\mathbf{q}, \omega) = \sigma_\alpha (\omega) \left(\mathbf{1} - \frac{D_\alpha (\omega)}{j\omega + D_\alpha (\omega) q^2} \mathbf{q}\mathbf{q} \right) . \quad (15)$$

The dielectric response of the material is determined not only by the drift and diffusion currents associated with the free carriers, but also by the polarization current stemming from the oscillations of the bound charges. In the following we will assume that the polarization response is local and isotropic (although a non-local polarization response can easily be accommodated),

$$\mathbf{J}^{\text{pol}} (\mathbf{r}, \omega) = j\omega \varepsilon_0 \chi_h \mathbf{E}(\mathbf{r}, \omega) = j\omega \varepsilon_0 (\varepsilon_h - 1) \mathbf{E}(\mathbf{r}, \omega) \quad (16)$$

where $\varepsilon_h = \chi_h + 1$ is the relative permittivity of the medium. From Ampère's law in the spatial transform domain, the complex effective permittivity that accounts for conduction and polarization is

$$\frac{\overline{\boldsymbol{\varepsilon}}_\alpha^{\text{pol+cond}} (\mathbf{q}, \omega)}{\varepsilon_0} = \mathbf{1} \varepsilon_h - j \frac{\overline{\boldsymbol{\sigma}}_\alpha}{\omega \varepsilon_0}$$

$$= \mathbf{1} \varepsilon_h - j \frac{\sigma_\alpha}{\omega \varepsilon_0} \left(\mathbf{1} - \frac{D_\alpha (\omega)}{j\omega + D_\alpha (\omega) q^2} \mathbf{q}\mathbf{q} \right)$$

$$= \mathbf{1} + \overline{\boldsymbol{\chi}}_\alpha^{\text{pol+cond}} (\mathbf{q}, \omega), \quad (17)$$

such that the complex effective susceptibility is

$$\overline{\boldsymbol{\chi}}_\alpha^{\text{pol+cond}} (\mathbf{q}, \omega) = \mathbf{1} (\varepsilon_h - 1) - j \frac{\sigma_\alpha}{\omega \varepsilon_0} \left(\mathbf{1} - \frac{D_\alpha (\omega)}{j\omega + D_\alpha (\omega) q^2} \mathbf{q}\mathbf{q} \right) . \quad (18)$$

In the next section we show that various forms of wire media have the same form for the permittivity, allowing the definition of an effective conductivity and diffusion coefficient for wire media.

For two charge species (e.g., electrons and ions),

$$\overline{\boldsymbol{\varepsilon}}^{\text{pol+cond}} (\mathbf{q}, \omega) = \mathbf{1} \varepsilon_h - j \frac{\overline{\boldsymbol{\sigma}}_{\text{elec}}}{\omega \varepsilon_0} - j \frac{\overline{\boldsymbol{\sigma}}_{\text{ions}}}{\omega \varepsilon_0}$$

$$= \overline{\boldsymbol{\varepsilon}}_{\text{elec}}^{\text{pol+cond}} (\mathbf{q}, \omega) + \overline{\boldsymbol{\varepsilon}}_{\text{ions}}^{\text{pol+cond}} (\mathbf{q}, \omega) - \mathbf{1} \varepsilon_h \quad (19)$$

where the interactions among charge species comes from $\mathbf{E}$ being the self-consistent field. We see later that for a double wire mesh system we obtain the same form for the permittivity.

It is also sometimes convenient to separate transverse and longitudinal components with respect to $\mathbf{q}$,

$$
\begin{aligned}
\frac{\overline{\overline{\varepsilon}}_\alpha^{\text{pol+cond}}(\mathbf{q}, \omega)}{\varepsilon_0} &= \left(\varepsilon_h - j\frac{\sigma_\alpha}{\omega\varepsilon_0}\right)(\mathbf{1} - \hat{\mathbf{q}}\hat{\mathbf{q}}) \\
&+ \left(\varepsilon_h - j\frac{\sigma_\alpha}{\omega\varepsilon_0}\left(1 - \frac{D_\alpha(\omega)q^2}{j\omega + D_\alpha(\omega)q^2}\right)\right)\hat{\mathbf{q}}\hat{\mathbf{q}} \\
&= \varepsilon_\alpha^T(\omega)(\mathbf{1} - \hat{\mathbf{q}}\hat{\mathbf{q}}) + \varepsilon_\alpha^L(q, \omega)\hat{\mathbf{q}}\hat{\mathbf{q}}. \quad (20)
\end{aligned}
$$

In particular, the above separation is useful in considering another example of a natural material for which spatial dispersion is important, an excitonic semiconductor (ESC), wherein excitons (quasi-particles) form from Coulomb-interacting electrons and holes that are bound into pair states. In this case the longitudinal dielectric function is [17], [18]

$$
\varepsilon^L(q) = \varepsilon_h + \frac{\omega_p^2}{\omega_T^2 - \omega(\omega - j\Gamma) + \gamma q^2} \quad (21)
$$

where $\gamma = \left(6.1728 \times 10^{-6}\omega_p^4/\varepsilon_h^4\right)^{1/3}$ and ω_T is the transition frequency (frequency to create the exciton). From (20), longitudinal fields satisfy

$$
\mathbf{D}_L = \varepsilon_0\left(\mathbf{1}\varepsilon_h - j\frac{\sigma^{\text{ESC}}}{\omega\varepsilon_0}\left(1 - \frac{D^{\text{ESC}}}{j\omega + D^{\text{ESC}}q^2}\mathbf{q}\mathbf{q}\right)\right) \cdot \mathbf{E}_L \quad (22)
$$

such that

$$
D_L = \varepsilon_0\varepsilon_h\left(1 + \frac{\frac{\sigma^{\text{ESC}}}{\varepsilon_h\varepsilon_0}}{j\omega + D^{\text{ESC}}q^2}\right)E_L. \quad (23)
$$

The constitutive relations implicit in (21) and (22) can be made to be the same if

$$
\sigma^{\text{ESC}} = \frac{j\omega\varepsilon_0\omega_p^2}{\omega_T^2 - \omega(\omega - j\Gamma)} \quad (24)
$$

$$
D^{\text{ESC}} = \frac{j\omega\gamma}{\omega_T^2 - \omega(\omega - j\Gamma)} = \frac{\gamma\sigma^{\text{ESC}}}{\omega_p^2\varepsilon_0}, \quad (25)
$$

wherein we identify the material's conductivity and diffusion parameter. In Section III these materials will be considered further.

Finally, taking the divergence of (4) and using the continuity equation and Gauss's law, we obtain the charge screening equation

$$
\left(\nabla^2 - k_{D,\alpha}^2\right)\rho_\alpha^s(\mathbf{r}) = 0 \quad (26)
$$

where

$$
k_{D,\alpha}^2 = \frac{j\omega\varepsilon + \sigma_\alpha}{D_\alpha\varepsilon} \quad (27)
$$

is essentially the square of the Debye wavenumber (usually the Debye wavenumber is defined for $\omega = 0$ such that $k_D = \sqrt{\sigma/D\varepsilon}$ [16], [19]). This wavenumber will be of interest in the following.

B. Artificial Materials

Maxwell's equations are linear, and so a time-harmonic current results in a time-harmonic field $(\mathbf{E}, \mathbf{B})$ from Ampère's and Faraday's laws, and a time-harmonic total charge ρ from
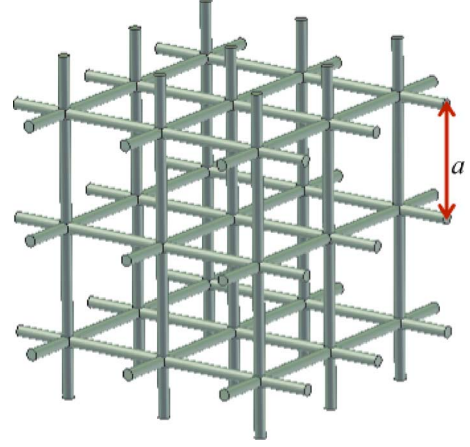

Fig. 1. Homogeneous, isotropic metamaterial consisting of a triple array of connected metal wires.

Gauss's law. However, as noted in the previous section, a time-harmonic current in a material region implicitly implies linearized charge transport. Furthermore, at the "microscopic" level for metamaterials (before homogenization, at the level of the constituent parts), it is usually assumed that $\mathbf{J} = \sigma\mathbf{E}$ for conductors, and $\mathbf{D} = \varepsilon\mathbf{E}$ for dielectrics. Therefore, in the microstructure of the material we are implicitly making the same assumptions as listed above for the simplified transport equation (since $\mathbf{J} = \sigma\mathbf{E}$ we are also ignoring diffusion in the microstructure, which for the case of metals is typically a very good approximation). From this starting point the metamaterial architecture (wire medium, split-ring resonator, etc.) is homogenized, which may lead to new properties not found in the constituent components, but which must be consistent with the microstructure assumptions (e.g., if we accounted for shear forces in the microstructure, we would have a different permittivity $\overline{\overline{\varepsilon}}(\mathbf{q}, \omega)$ for the metamaterial).

In the following we show that various wire mediums can be modeled by a drift-diffusion equation at the macroscopic level, in terms of effective parameters that implicitly arise from the particular model of the microstructure. In the appendix we present the coupled integral-differential equations that describe scattering and resonator problems based on this approach.

1) Isotropic Connected Wire Mesh: Consider a connected isotropic wire medium (CIWM) as depicted in Fig. 1, constructed from imperfectly-conducting wires characterized by $\varepsilon_m = 1 - \omega_m^2/(\omega(\omega - j\Gamma))$, where ω_m and Γ are the plasma frequency and damping frequency of the metal, respectively.

The permittivity of the homogenized medium is [20]

$$
\frac{\overline{\overline{\varepsilon}}^{\text{CIWM}}(\mathbf{q}, \omega)}{\varepsilon_0} = \mathbf{1}\varepsilon_h - \kappa\left(1 - \frac{1}{q^2 + l_0\left(\frac{\varepsilon_h k_p^2}{\varepsilon_m - \varepsilon_h}\frac{1}{f_v} - k_h^2\right)}\mathbf{q}\mathbf{q}\right) \quad (28)
$$

where

$$
\kappa = \left(\frac{k_0^2}{k_p^2} - \frac{1}{\varepsilon_m - \varepsilon_h}\frac{1}{f_v}\right)^{-1} \quad (29)
$$

$f_v = \pi r^2/a^2$ is the volume fraction of the wires (r is the wire radius, a is the wire period), $k_h = \omega\sqrt{\mu_0\varepsilon_0\varepsilon_h} = k_0\sqrt{\varepsilon_h}$

is the wavenumber in the host medium, $k_p = \omega_p/c$ is the plasma wavenumber ($(k_p a)^2 \cong 2\pi/\ln(a^2/4r_w(a-r)) \cong 2\pi/(\ln(a/2\pi r)+0.5275)$; see [20, (11)] for the exact expression), and $l_0 = 3/\left(1 + 2k_p^2/\beta_1^2\right)$, where

$$\frac{1}{\beta_1^2} = 2\left(\frac{a}{2\pi}\right)^2 \sum_{n=1}^{\infty} \frac{\left[J_0\left(\frac{2\pi r}{a}n\right)\right]^2}{n^2} \qquad (30)$$

and where J_0 is the zeroth-order Bessel function. As discussed in [20], this expression is very accurate below the effective plasma frequency. For $\varepsilon_h \sim 1$ the effective plasma frequency is

$$\frac{1}{\omega_{p,eff}^2} = \varepsilon_h \left(\frac{1}{\omega_m^2 f_v} + \frac{1}{k_p^2 c^2}\right) \qquad (31)$$

although if ε_h differs considerably from unity the effective transverse permittivity is not Drude-like and the effective plasma frequency is given by a quadratic form obtained from setting the transverse permittivity to zero. For $\varepsilon_h \sim 1$ the effective plasma frequency $f_{p,eff}$ is in the low THz except for the very thinnest wires. The isotropic wire medium permittivity (28) reduces to the simpler form [21]

$$\frac{\overline{\overline{\varepsilon}}^{\text{CIWM,PEC}}(\mathbf{q}, \omega)}{\varepsilon_0} = \mathbf{1}\varepsilon_h - \frac{k_p^2}{k_0^2}\left(\mathbf{1} - \frac{1}{q^2 - l_0 k_h^2}\mathbf{q}\mathbf{q}\right) \qquad (32)$$

when $|\varepsilon_m| \to \infty$, i.e., as the wire conductivity becomes infinite.

Equating (17) to (28) we see that the connected wire medium can be represented by a drift-diffusion model

$$\left(\mathbf{1} - \frac{D^{\text{CIWM}}}{j\omega}\nabla\nabla\right) \cdot \mathbf{J}^{\text{cond}}(\mathbf{r}, \omega) = \sigma^{\text{CIWM}}\mathbf{E}(\mathbf{r}, \omega) \qquad (33)$$

for effective conduction current, with effective conductivity and diffusion coefficient

$$\sigma^{\text{CIWM}} = \frac{-j\omega\varepsilon_0}{\left(\frac{k_0^2}{k_p^2} - \frac{1}{\varepsilon_m - \varepsilon_h}\frac{1}{f_v}\right)} \quad \frac{\text{S}}{\text{m}} \qquad (34)$$

$$D^{\text{CIWM}} = \frac{j\omega}{l_0\left(\frac{\varepsilon_h k_p^2}{\varepsilon_m - \varepsilon_h}\frac{1}{f_v} - k_h^2\right)} = \frac{\sigma^{\text{CIWM}}}{l_0\varepsilon_0\varepsilon_h k_p^2} \quad \frac{\text{m}^2}{\text{s}}. \qquad (35)$$

For perfectly-conducting wires,

$$\sigma^{\text{CIWM,PEC}} = \frac{-j\omega\varepsilon_0 k_p^2}{k_0^2} = \frac{k_p^2}{j\omega\mu_0}$$

$$D^{\text{CIWM,PEC}} = \frac{-j\omega}{l_0 k_h^2} = \frac{v_h^2}{j\omega l_0} \qquad (36)$$

where $v_h = 1/\sqrt{\mu_0\varepsilon_0\varepsilon_h}$ is the phase velocity in the nondispersive host. Note that $\sigma^{\text{CIWM,PEC}}$ is pure imaginary, and so this effective conductivity represents an inductive effect due to the PEC wires. The diffusion coefficient $D^{\text{CIWM,PEC}}$ is also pure imaginary, and, comparing to (11), is analogous to the case $\omega\tau \gg 1$ for natural materials. In the PEC case the diffusion coefficient is insensitive to varying the wire medium period a and weakly sensitive to the value of r/a. The effective conductivity is sensitive to the wire medium parameters via the plasma frequency.
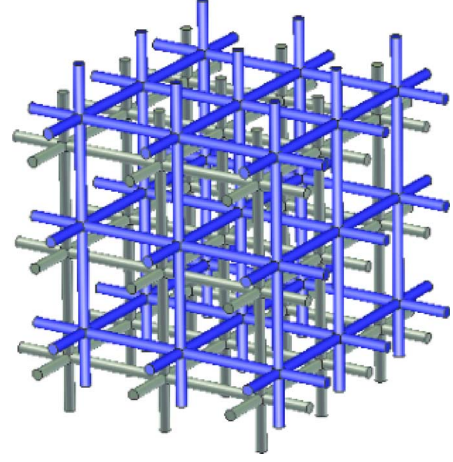

Fig. 2. Homogeneous, isotropic metamaterial consisting of two wire meshes of triply-connected metal wires. The distance between the two nonconnected networks is $a/2$.

To complete the analogy, for lossless materials (plasma or metals), (4) can be written as

$$j\omega\mathbf{J}_\alpha^{\text{cond}}(\mathbf{r}, \omega) + \frac{\langle v^2 \rangle}{3}\nabla\rho_\alpha^s(\mathbf{r}, \omega) - \omega_p^2\varepsilon_0\mathbf{E}(\mathbf{r}, \omega) = 0 \quad (37)$$

where $\omega_p^2 = q^2 N/m\varepsilon_0$ is the square of the plasma frequency and v is the appropriate electron velocity, v_{thermal} for plasma or v_F for good metals. The analogous transport equation for a PEC wire mesh is

$$j\omega\mathbf{J}^{\text{cond}}(\mathbf{r}, \omega) + \frac{v_h^2}{l_0}\nabla\rho_\alpha^s(\mathbf{r}, \omega) - \omega_p^2\varepsilon_0\mathbf{E}(\mathbf{r}, \omega) = 0 \quad (38)$$

where $l_0 = 2.3$ is a typical value. Capacitive loads can be used to reduce or eliminate spatial dispersion in wire media [7], [22], although this effect is not considered here.

2) Isotropic Connected Double Wire Mesh: An alternative topology for the wire mesh network, which in a certain sense generalizes the one discussed in the previous sub-section, is depicted in Fig. 2. This metamaterial consists of two independent networks (mesh A and mesh B), with each network being an isotropic connected wire mesh, analogous to the one shown in Fig. 1. The period of each wire mesh is a. The electrodynamics of this artificial medium were discussed in [23], where it was argued that the effective medium is non-Maxwellian in the sense that in the low-frequency limit it may support more than two plane waves for a fixed direction of propagation. However, no model for the effective dielectric response was proposed in [23]. This will be done in what follows.

The general calculation of the effective response of the isotropic connected double wire mesh is not a simple matter, because the two wire meshes can be strongly coupled. Here, we restrict our attention to the case in which the wire meshes are interleaved in such a manner that the distance between adjacent wires in the different meshes is $a/2$. Moreover, for simplicity, we only discuss the case wherein the host material is air ($\varepsilon_h = 1$), and the wires are PEC.

For a given external excitation, let $\mathbf{j}_{d,A}$ and $\mathbf{j}_{d,B}$ represent the microscopic (conduction) currents in mesh A and B, respectively. The macroscopic (averaged) polarization current associated with mesh A is thus $\mathbf{J}_{d,A} = j\omega\mathbf{P}_A^{\mathrm{cond}} = \langle\mathbf{j}_{d,A}\rangle$, where $\langle\ \rangle$ is an operator that performs a spatial averaging ($\mathbf{J}_{d,B} = j\omega\mathbf{P}_B^{\mathrm{cond}}$ is defined in the same manner). The operator $\langle\ \rangle$ may represent, for example, an ideal low pass spatial filter that removes the fluctuations of the fields that occur in a scale smaller than the unit cell [24]. In general, the microscopic currents induced in mesh A ($\mathbf{j}_{d,A}$) depend on the currents induced in mesh B ($\mathbf{j}_{d,B}$). Since in our case the two meshes are (from a geometrical point of view) as far as possible from each other, it is reasonable to suppose that the fields radiated by the currents in mesh A, $\mathbf{j}_{d,A}$, calculated over mesh B, are approximately the same as the fields that would be radiated by the macroscopic current distribution associated with mesh A, $\mathbf{J}_{d,A}$. Notice that such an assumption is equivalent to stating that the two meshes are not very strongly coupled in the near-field, so that the influence of one mesh on the other can be regarded as a macroscopic excitation.

But for any macroscopic external excitation, we know that the macroscopic response of the mesh A is such that $\mathbf{P}_A^{\mathrm{cond}} = \left(\overline{\boldsymbol{\varepsilon}}^A - \varepsilon_0\mathbf{1}\right)\cdot\mathbf{E}$ where $\mathbf{E}$ represents the macroscopic (spatially averaged) electric field, and $\overline{\boldsymbol{\varepsilon}}^A$ is the effective dielectric function of mesh A (when mesh B is absent). Similarly, under the same conditions, we have $\mathbf{P}_B^{\mathrm{cond}} = \left(\overline{\boldsymbol{\varepsilon}}^B - \varepsilon_0\mathbf{1}\right)\cdot\mathbf{E}$, where $\overline{\boldsymbol{\varepsilon}}^B$ is the effective dielectric function of mesh B (when mesh A is absent). Therefore, since $\mathbf{P}_A^{\mathrm{cond}}+\mathbf{P}_B^{\mathrm{cond}} = \left(\overline{\boldsymbol{\varepsilon}}^A + \overline{\boldsymbol{\varepsilon}}^B - 2\varepsilon_0\mathbf{1}\right)\cdot\mathbf{E}$, the effective response of the system formed by mesh A and mesh B is simply

$$\overline{\boldsymbol{\varepsilon}}^{A+B} = \overline{\boldsymbol{\varepsilon}}^A + \overline{\boldsymbol{\varepsilon}}^B - \varepsilon_0\mathbf{1}. \tag{39}$$

We emphasize that the derived result is exact under the assumption that the action of one mesh on the other can be seen as a macroscopic excitation, or equivalently that only the smooth (slowly varying) part of the fields radiated by one of the meshes influences the currents on the other mesh. It should be clear that the derived result is the metamaterial analogue of the dielectric function of a natural material with a conductive response determined by carriers of two species, (19). Obviously, we may rewrite the effective dielectric function as

$$\frac{\overline{\boldsymbol{\varepsilon}}^{A+B}}{\varepsilon_0} = \varepsilon_t\left(\omega\right)\left(\mathbf{1} - \frac{\mathbf{q}\mathbf{q}}{q^2}\right) + \varepsilon_l\left(\omega,q\right)\frac{\mathbf{q}\mathbf{q}}{q^2} \tag{40}$$

where,

$$\varepsilon_t\left(\omega\right) = 1 - \frac{k_{pA}^2}{\frac{\omega^2}{c^2}} - \frac{k_{pB}^2}{\frac{\omega^2}{c^2}} \tag{41}$$

and

$$\varepsilon_l\left(\omega,q\right) = 1 + \frac{k_{pA}^2}{\frac{q^2}{l_{0A}} - \frac{\omega^2}{c^2}} + \frac{k_{pB}^2}{\frac{q^2}{l_{0B}} - \frac{\omega^2}{c^2}} \tag{42}$$

where k_{pA} and k_{pB} are the plasma wavenumbers of mesh A and B, respectively, and l_{0A} and l_{0B} are the parameters that characterize the effects of spatial dispersion. These parameters are defined consistently with the formulas of Section II-B.I, and depend on the values of the wire radii (r_A and r_B), which can

be different for the two wire meshes. Evidently, the transverse permittivity (41) can be recast into the simpler form

$$\varepsilon_t\left(\omega\right) = 1 - \frac{k_{p,eff}^2}{\frac{\omega^2}{c^2}}, \quad \text{with } k_{p,eff} = \sqrt{k_{p,A}^2 + k_{p,B}^2}. \tag{43}$$

The wave number $k_{p,eff}$ is the effective plasma wave number, which is always higher than the plasma wave numbers of the individual networks, as a result of their electromagnetic coupling.

3) Isotropic Non-Connected Wire Medium: We can also consider a non-connected isotropic wire medium (NCIWM), where the wires do not intersect [21]. The homogenized permittivity in this case, for perfectly conducting wires, is

$$\frac{\overline{\boldsymbol{\varepsilon}}^{\mathrm{NCIWM}}\left(\mathbf{q},\omega\right)}{\varepsilon_0} = \mathbf{1}\varepsilon_h - \varepsilon_h k_p^2 \sum_{\alpha=x,y,z}\frac{\widehat{\boldsymbol{\alpha}}\widehat{\boldsymbol{\alpha}}}{k_h^2 - q_\alpha^2}. \tag{44}$$

This case does not fit a simple isotropic diffusion model (9), but it does fit three scalar diffusion equations. For example, consider a z-directed wire and assume $\mathbf{J} = \widehat{\mathbf{z}}J_z$, such that

$$\nabla \cdot \mathbf{J} = \frac{\partial J_z}{\partial z} = -j\omega\rho = -j\omega\rho_z \tag{45}$$

where ρ_z is charge density in the z-directed wire. Then, the drift-diffusion equation is

$$J_z = \sigma_z E_z - D_z\widehat{\mathbf{z}}\cdot\nabla\rho_z = \sigma_z E_z - D_z\frac{\partial\rho_z}{\partial z}$$
$$= \sigma_z E_z + \frac{D_z}{j\omega}\frac{\partial^2 J_z}{\partial z^2} \tag{46}$$

such that

$$J_z = \frac{\sigma_z}{1 + \frac{D_z}{j\omega}q_z^2}E_z. \tag{47}$$

Repeating for wires along the other coordinate directions and equating to (44),

$$\sigma_x = \sigma_y = \sigma_z = \sigma^{\mathrm{NCIWM}} = -j\omega\varepsilon_0\varepsilon_h\frac{k_p^2}{k_h^2} = \sigma^{\mathrm{CIWM,PEC}}$$
$$D_x = D_y = D_z = D^{\mathrm{NCIWM}} = \frac{-j\omega}{k_h^2} = l_0 D^{\mathrm{CIWM}}. \tag{48}$$

The effective conductivity of the connected and non-connected wire mediums are the same, but the diffusion coefficients differ by a factor l_0 of order one. Therefore, the non-connected wire medium effective permittivity is

$$\frac{\overline{\boldsymbol{\varepsilon}}^{\mathrm{pol+cond}}\left(q_z,\omega\right)}{\varepsilon_0} = \mathbf{1}\varepsilon_h + \frac{\sigma^{\mathrm{NCIWM}}}{\varepsilon_0}\sum_{\alpha=x,y,z}\frac{\widehat{\boldsymbol{\alpha}}\widehat{\boldsymbol{\alpha}}}{j\omega + D^{\mathrm{NCIWM}}q_\alpha^2}.$$

4) Anisotropic Uniaxial Wire Medium: For a uniaxial wire medium (UWM) consisting of unidirectional, perfectly-conducting parallel wires, as depicted in Fig. 3 the homogenized permittivity is [5]

$$\underline{\boldsymbol{\varepsilon}}^{\mathrm{UWM}}\left(q\right) = \varepsilon_0\varepsilon_h\left(\widehat{\mathbf{x}}\widehat{\mathbf{x}} + \widehat{\mathbf{y}}\widehat{\mathbf{y}} + \widehat{\mathbf{z}}\widehat{\mathbf{z}}\varepsilon_{zz}\left(q_z\right)\right) \tag{49}$$

where

$$\varepsilon_{zz}\left(q_z\right) = 1 - \frac{k_p^2}{k_h^2 - q_z^2}. \tag{50}$$

TABLE I
COMPARISON BETWEEN CONDUCTIVITY AND DIFFUSION CONSTANTS FOR VARIOUS NATURAL AND ARTIFICIAL MATERIALS $f = 10$ GHz

Material	f_p (THz)	σ (S/m)	Dk_0^2 (1/s)	$k_D = \sqrt{\frac{j\omega\varepsilon+\sigma}{D\varepsilon}}$ (m^{-1})	$(k_D\lambda_0)^{-1} = L_D/\lambda_0$
gold	2180.94	$3.3 \times 10^7 - j4.2 \times 10^4$	$341.56 - j0.43$	$2.19 \times 10^{10} + j183.83$	$1.52 \times 10^{-9} - j1.27 \times 10^{-17}$
SC ($N = 10^{20}$m^{-3})	0.176	$2.33 - j0.00316$	$165.58 - j2.24$	$3.41 \times 10^6 + j2.45 \times 10^6$	$6.46 \times 10^{-6} - j4.64 \times 10^{-6}$
SC ($N = 10^{22}$m^{-3})	1.76	$233.63 - j3.16$	$165.58 - j2.24$	$2.41 \times 10^7 + j3.45 \times 10^5$	$1.38 \times 10^{-6} - j1.97 \times 10^{-8}$
SC ($N = 10^{24}$m^{-3})	17.6	$2.33 \times 10^4 - j316.49$	$165.58 - j2.24$	$2.42 \times 10^8 + j3.45 \times 10^4$	$1.38 \times 10^{-7} - j1.97 \times 10^{-11}$
CIWM	0.022	$7.11 \times 10^{-4} - j2.73$	$7.13 \times 10^6 - j2.73 \times 10^{10}$	$627 + j0.021$	$0.053 - j1.78 \times 10^{-6}$
PEC CIWM	0.022	$-j2.73$	$-j2.73 \times 10^{10}$	627.08	0.053
PEC NCIWM	0.022	$-j2.73$	$-j6.28 \times 10^{10}$	413.88	0.081

TABLE II
COMPARISON BETWEEN CONDUCTIVITY AND DIFFUSION CONSTANTS FOR VARIOUS NATURAL AND ARTIFICIAL MATERIALS AT $f = 1$ THz

| Material	σ (S/m)	Dk_0^2 (1/s)	$k_D = \sqrt{\frac{j\omega\varepsilon+\sigma}{D\varepsilon}}$ (m^{-1})	$(k_D\lambda_0)^{-1} = L_D/\lambda_0$
gold	$3.3 \times 10^7 - j4.2 \times 10^6$	$3.36 \times 10^6 - j4.23 \times 10^5$	$2.20 \times 10^{10} + j1.84 \times 10^4$	$1.52 \times 10^{-7} - j1.27 \times 10^{-13}$
SC ($N = 10^{20}$m^{-3})	$0.82 - j1.12$	$5.84 \times 10^5 - j7.91 \times 10^5$	$1.65 \times 10^7 + j5.03 \times 10^7$	$1.97 \times 10^{-5} - j5.99 \times 10^{-5}$
SC ($N = 10^{22}$m^{-3})	$82.42 - j111.65$	$5.84 \times 10^5 - j7.91 \times 10^5$	$1.85 \times 10^7 + j4.49 \times 10^7$	$2.62 \times 10^{-5} - j6.34 \times 10^{-5}$
SC ($N = 10^{24}$m^{-3})	$8.24 \times 10^3 - j1.11 \times 10^4$	$5.84 \times 10^5 - j7.91 \times 10^5$	$2.37 \times 10^8 + j3.52 \times 10^6$	$1.41 \times 10^{-5} - j2.09 \times 10^{-7}$
CIWM	$7.06 - j271.51$	$7.08 \times 10^{10} - j2.72 \times 10^{12}$	$6.27 \times 10^4 + j209.87$	$0.053 - j1.78 \times 10^{-4}$
PEC CIWM	$-j272.58$	$-j2.73 \times 10^{12}$	6.27×10^4	0.053
PEC NCIWM	$-j272.58$	$-j6.28 \times 10^{12}$	4.14×10^4	0.081
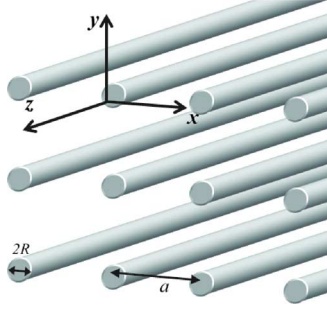
Fig. 3. Anisotropic wire medium.

This is the same as for the nonconnected wire medium, except for the absence of the terms involving q_x and q_y. Therefore,

$$\frac{\overline{\varepsilon}^{\text{UWM}}(q_z, \omega)}{\varepsilon_0} = \mathbf{1}\varepsilon_h + \frac{\sigma^{\text{NCIWM}}}{\varepsilon_0} \frac{\widehat{\mathbf{z}}\widehat{\mathbf{z}}}{j\omega + D^{\text{NCIWM}}q_z^2}. \quad (51)$$

For imperfectly-conducting wires characterized by ε_m in air ($\varepsilon_h = 1$), k_h^2 is replaced by $k_0^2 - j\xi k_0$, where

$$\xi = \frac{(k_p a)^2}{j\omega\pi r^2 \sqrt{\mu_0\varepsilon_0}(\varepsilon_m - 1)} \quad (52)$$

is related to loss [22], with a corresponding change to the expressions for σ and D. The same expression applies to carbon nanotubes with a change in the value of ξ [25].

III. COMPARISON OF TRANSPORT PROPERTIES OF NATURAL AND ARTIFICIAL MATERIALS: QUANTITATIVE MEASURE OF SPATIAL DISPERSION

It was shown in the previous sections that plasmas, semiconductors (and metals in the hydrodynamic approximation), and various forms of wire metamaterials can be represented in a common transport/drift-diffusion framework. It is worth noting that the diffusion coefficient itself provides a measure of the importance of non-locality, since in the limit $D \to 0$ the material is local. Since artificial materials often have significant spatial dispersion effects at relatively low frequencies, it is worthwhile to compare the conductivity and diffusion coefficient for some representative materials, both natural and artificial. The conductivity and diffusion coefficient for semiconductors and plasmas are given in (11).

In the following, for semiconductors (SC) we assume $T = 300$ K, $m = 0.26m_e$, $\varepsilon_h = 12$ and $\tau = 2.16 \times 10^{-13}$ s. For metal we assume gold, with $\tau = 2 \times 10^{-14}$ s, $N = 5.9 \times 10^{28}$ m^{-3}, and $v_F = \hbar \left(3N\pi^2\right)^{1/3}/m_e = 1.4 \times 10^6$ m/s. For the wire medium (connected (CIWM) and non-connected (NCIWM); perfectly conducting wires are denoted by PEC)) we assume $\varepsilon_h = 1$, $a = \lambda_0/10$ and $r = a/100$, so that $k_p a = 1.39$ ($k_p = 2.21k_0$). For the imperfectly-conducting wires, $\varepsilon_m = 1 - \omega_m^2/(\omega(\omega - j\Gamma))$ where $\omega_m = 1.37 \times 10^{16}$ s^{-1} and $\Gamma = 5 \times 10^{13}$ s^{-1}. Table I shows results at $f = 10$ GHz, and Table II at $f = 1$ THz.

It can be seen that the normalized diffusion coefficient Dk_0^2 is relatively small for the semiconductor and gold materials, and relatively large and imaginary for the wire media, thus confirming the importance of spatial dispersion for wire media. However, more important than the individual σ and D values is the Debye wavenumber k_D, (27), which is associated with charge screening and which occurs in the longitudinal problem described in Section V, discussed later. The Debye length is $L_D = k_D^{-1}$, and the Debye length normalized to wavelength is shown in the tables. The real-part of the Debye length provides a measure of the distance over which fields are screened by mobile charges. It can be seen that for the wire media, fields are not screened well (although as a decreases, screening improves as shown in Section V), leading to important spatial dispersion/diffusion effects well into the bulk of the material (at least hundreds of wavelengths into the material). For the natural materials listed in the tables and macroscopic size regions, diffusion effects will only be important very near the material boundaries, but for nanoscopic material regions diffusion can influence fields in the interior (shown in the example in Section V).

TABLE III
EFFECTIVE PARAMETERS FOR ZnSe NEAR THE PLASMA FREQUENCY

Material	ω/ω_p	σ(S/m)	Dk_0^2(1/s)	$k_D = \sqrt{\frac{j\omega\varepsilon+\sigma}{D\varepsilon}}$(m^{-1})	$(k_D\lambda_0)^{-1} = L_D/\lambda_0$
ZnSe	0.8	$j12.35$	$1.46 \times 10^5 + j2.45 \times 10^{11}$	$2.71 \times 10^7 + j8.06$	1.23×10^{-4}
ZnSe	1.2	$j18.58$	$7.41 \times 10^5 + j8.26 \times 10^{11}$	$2.71 \times 10^7 + 12.08$	1.23×10^{-4}

TABLE IV
EFFECTIVE PARAMETERS FOR ZnSe NEAR THE TRANSITION FREQUENCY

Material	ω/ω_T	σ(S/m)	Dk_0^2(1/s)	$k_D = \sqrt{\frac{j\omega\varepsilon+\sigma}{D\varepsilon}}$(m^{-1})	$(k_D\lambda_0)^{-1} = L_D/\lambda_0$
ZnSe	0.8	$0.01 + j460.58$	$3.68 \times 10^{10} + j1.66 \times 10^{15}$	$1.64 \times 10^7 + j179.56$	2.03×10^{-4}
ZnSe	1.2	$0.02 - j564.78$	$1.25 \times 10^{11} - j4.57 \times 10^{15}$	$246.94 + j1.79 \times 10^7$	$-j1.86 \times 10^{-4}$

For the case of the excitonic semiconductor ZnSe, $\varepsilon_h = 8.01$, $\omega_T = 4.25 \times 10^{15}$ s^{-1}, $\Gamma = 10^{-5}\omega_T$, and $\omega_p = 0.07416\omega_T = 3.15 \times 10^{14}$ s^{-1}. Table III shows the effective conductivity and diffusion coefficient near the plasma frequency, and Table IV shows the same quantities near the exciton transition frequency.

It can be seen that the diffusion coefficient is very large for the excitonic semiconductor, similar to the wire medium case, in agreement with the well-known fact that spatial dispersion is important for these materials.

IV. ADDITIONAL BOUNDARY CONDITIONS

In any realistic problem of wave propagation involving either natural or structured materials one needs to consider the effect of interfaces, and in particular in the framework of macroscopic electrodynamics it is essential to know how the macroscopic fields are coupled in different media. In a local, isotropic medium, two plane waves may propagate, and the usual boundary conditions on tangential electric and magnetic fields are sufficient to solve for fields in regions of space containing heterogeneous materials. However, in non-local materials additional waves may propagate, necessitating the use of additional boundary conditions (ABCs) when solving problems involving interfaces. In the literature, many ABCs have been proposed. In the following, we show that one of the earliest ABCs, proposed by Pekar for excitonic semiconductors [26], is identical to the ABC usually used for plasmas and semiconductors, and even, if properly applied, to the newly developed ABCs for wire media. Furthermore, this condition follows from the usual boundary condition on current, and thus can be derived from elementary electromagnetics. With a slight change in notation, we propose this ABC for general materials when one additional boundary condition is necessary, and provided it is expected from microscopic considerations that the current associated with mobile carriers vanishes at the pertinent interface (which is not always the case; e.g., the condition holds neither for a wire medium attached to a metallic plate, nor for a semi-infinite wire medium embedded in a semiconductor).

The susceptibility (18) leads to the polarization response

$$\mathbf{P}^{\text{pol+cond}} = \varepsilon_0 \left(\mathbf{1}\,(\varepsilon_h - 1) - j\frac{\sigma}{\omega\varepsilon_0}\left(1 - \frac{D}{j\omega + Dq^2}\mathbf{q}\mathbf{q}\right) \right) \cdot \mathbf{E}$$
$$= \mathbf{P}^{\text{local,pol}} + \mathbf{P}^{\text{local,cond}} + \mathbf{P}^{\text{nonlocal,cond}}$$
$$= \mathbf{P}^{\text{local,pol}} + \mathbf{P}^{\text{cond}}, \qquad (53)$$

where we separate out the polarization response from the conduction charge response. Although the differentiation between bound and unbound (free, conduction) charge is somewhat artificial from a macroscopic point of view at nonzero frequencies, in what follows it remains a useful idea. For a natural material, $\mathbf{P}^{\text{cond}}$ represents the response of "mobile" charges associated with the conductivity of the medium. For an artificial wire material, σ is an effective parameter, but we can still divide the response into a local polarization response and everything else, which we will call conduction.

In 1957 Pekar proposed an additional boundary condition for excitonic semiconductors, such that the excitonic part of polarization, i.e., the contribution to the polarization related exclusively to excitons, should go to zero at the boundary with a dielectric,

$$\mathbf{P}^{\text{exciton}} = \mathbf{P} - \varepsilon_0\,(\varepsilon_h - 1)\,\mathbf{E} = 0. \qquad (54)$$

The condition is applied inside the material, and leads to two ABCs (for the parallel and perpendicular components). When only one ABC is needed, a natural condition is that the normal component of excitonic polarization goes to zero at the boundary, which is

$$\mathbf{n} \cdot \mathbf{P}^{\text{exciton}} = \mathbf{n} \cdot \mathbf{P} - \varepsilon_0\,(\varepsilon_h - 1)\,\mathbf{n} \cdot \mathbf{E} = 0. \qquad (55)$$

In this case, excitons are the only mobile charges (at the frequencies of exciton absorption). From (53), the above condition is the same as

$$\mathbf{n} \cdot \left(\mathbf{P}^{\text{pol+cond}} - \mathbf{P}^{\text{local,pol}}\right) = \mathbf{n} \cdot \mathbf{P}^{\text{cond}} = 0 \qquad (56)$$

which makes sense physically since the presence of diffusion will not allow a singular surface of mobile charges. Although widely used for excitonic materials, we show below that the Pekar condition (56) condition is actually quite general, and applies in many cases to both natural materials (plasma and semiconductors) and wire media.

For natural semiconductors and plasmas, the usual ABC is that total (local plus nonlocal) conduction current goes to zero at an interface with a dielectric [27]–[30]. This is clearly the same as (56). For an array of parallel wires (uniaxial wire medium), the ABC is that conduction current at the ends of the wires goes to zero at the boundary with a dielectric [31]. This also holds for other more complex topologies of connected [20] and non-connected [32] wire mesh mediums. Specifically, in general for each sub-lattice of parallel wires that is severed at the interface

one is required to impose that $\mathbf{P} \cdot \widehat{\boldsymbol{\alpha}} = 0$, where $\mathbf{P}$ is the polarization vector associated exclusively with the conduction currents and $\widehat{\boldsymbol{\alpha}}$ is a unit vector that determines the direction of the considered sub-lattice of wires [32]. For the case of a 1D-wire medium this is equivalent to the homogenized fields satisfying the condition [31]

$$\varepsilon_{out}\mathbf{n} \cdot \mathbf{E}^{\text{outside}} = \varepsilon_h \mathbf{n} \cdot \mathbf{E}^{\text{inside}} \qquad (57)$$

where ε_{out} is the relative permittivity of the non-conducting exterior medium. Next we show that (57) is the same as (56).

Writing on either side of the boundary

$$\mathbf{D} = \varepsilon_0 \mathbf{E} + \mathbf{P} = \varepsilon_0 \mathbf{E} + \mathbf{P}^{\text{local,pol}} + \mathbf{P}^{\text{cond}} = \varepsilon_0 \varepsilon_r \mathbf{E} + \mathbf{P}^{\text{cond}}$$

(using $\mathbf{P}^{\text{local,pol}} = \varepsilon_0 \left(\varepsilon_r - 1 \right) \mathbf{E}$), and using the fact that normal $\mathbf{n} \cdot \mathbf{D} = D_n$ is continuous across the boundary,

$$\varepsilon_0 \varepsilon_{out} E_n^{\text{outside}} + P_n^{\text{cond,outside}} = \varepsilon_0 \varepsilon_h E_n^{\text{inside}} + P_n^{\text{cond,inside}}. \qquad (58)$$

Assuming that the outside region is nonconducting $P_n^{\text{cond,outside}} = 0$, and setting $P_n^{\text{cond,inside}} = 0$ at the boundary we have

$$\varepsilon_{out} E_n^{\text{outside}} = \varepsilon_h E_n^{\text{inside}} \qquad (59)$$

which is the wire medium ABC. For $\varepsilon_h = \varepsilon_{out} = 1$ this is the same as continuity of normal $\mathbf{E}$. Therefore, we propose that Pekar's ABC for "conductive" polarization is quite general, and applies to plasmas (and metals in the hydrodynamic limit), semiconductors, and wire media adjacent to another medium that cannot sustain the flow of the mobile carriers.

Furthermore, the ABC (56) can be derived from the well-known large-scale form of the continuity equation,

$$\mathbf{n} \cdot \left(\mathbf{J}_2^{\text{cond}} - \mathbf{J}_1^{\text{cond}} \right) = -\nabla_s \cdot \mathbf{J}_s^{\text{cond}} - j\omega \rho_s \qquad (60)$$

where $\mathbf{J}_s^{\text{cond}}$ is a surface current and ρ_s is a surface charge, neither associated with bound-charge polarization. If both regions have finite conductivity (including zero conductivity), then $\mathbf{J}_s^{\text{cond}} = \mathbf{0}$. In the presence of diffusion, a surface charge can not exist (physically, this makes sense, and mathematically, if ρ were singular then $\nabla\rho$ would have a higher-order singularity that is not present in $\mathbf{J}^{\text{cond}}$ or $\mathbf{E}$ in the drift-diffusion equation (e.g., (9)). Thus, $\mathbf{n} \cdot \left(\mathbf{J}_2^{\text{cond}} - \mathbf{J}_1^{\text{cond}} \right) = 0$. If the outside region is a dielectric, then $\mathbf{n} \cdot \mathbf{J}^{\text{cond}} = 0$, which is the same as (56). Therefore, the Pekar condition (56) is essentially the well-known condition on normal conduction current assuming the presence of diffusion.

The previous discussion was for exterior mediums that are non-conducting. Particularly for a uniaxial wire medium the case of termination in a ground plane is of interest. In this case, rather than $P_n^{\text{cond}} = 0$ ($J_n = 0$) at the interface, for a PEC ground plane the microscopic boundary condition is [8], [33]–[35]

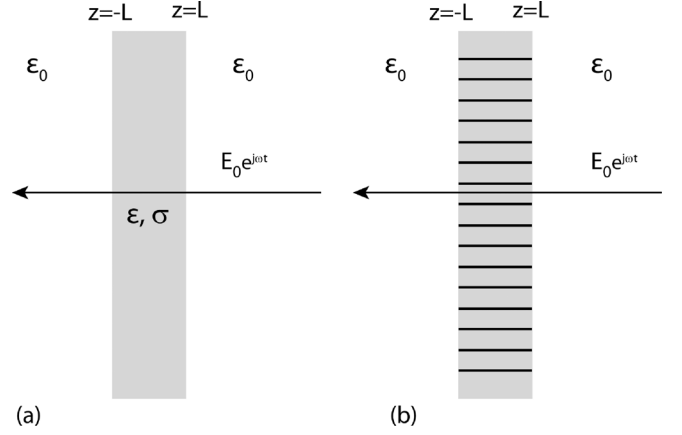$$\frac{\partial}{\partial n} J_n = 0 \qquad (61)$$

Fig. 4. Planar slab medium with impressed quasi-static field. (a) natural material, (b) wire medium.

which is the same as $\partial P_n^{\text{cond}} / \partial n = 0$. Furthermore, for a wire medium terminated at an imperfectly-conducting thin plane characterized by a surface conductivity σ_{2d}, the boundary condition is [36]

$$J_n + \frac{\sigma_{2d}}{j\omega\varepsilon_0\varepsilon_r} \frac{\partial J_n}{\partial n} = 0. \qquad (62)$$

Thus, we can write a more general ABC as

$$\left(\alpha + \beta \frac{\partial}{\partial n} \right) \mathbf{n} \cdot \mathbf{P}^{\text{cond}} = 0 \qquad (63)$$

where $\alpha = 1$ and $\beta = 0$ for a nonconducting exterior medium, $\alpha = 0$ and $\beta = 1$ for a wire medium connected to a PEC plane, and $\alpha = 1$ and β is a constant for a wire medium terminated in an imperfect conductor. The condition (63) has also been proposed as a generalization of Pekar's condition for excitonic semiconductors [2, p. 353]. Other generalized additional boundary conditions that apply to the case where the wire medium is terminated with lumped loads were formulated in [37].

V. Longitudinal Excitation Example

As an example of the above ideas, we consider a planar slab of material excited by a purely longitudinal (with respect to the slab normal) impressed field, like what would be found between the plates of a capacitor. Since such a dynamical field is not a free solution of Maxwell's equations, in general it may need to be created by some distributed source, or it can be considered as a quasi-static excitation.

The slab has width $2L$, and is immersed in vacuum. Fig. 4(a) depicts a natural material characterized by ε, σ, and D, and Fig. 4(b) depicts a wire medium (before homogenization), consisting of parallel wires. For this excitation, the three-dimensional wire mesh (connected or nonconnected) provides the same response.

Starting with the general form of susceptibility in wavevector space (18), we assume for generality the case of two charge species (19) or a double mesh wire medium (39)–(40),

$$\overline{\chi}\left(\mathbf{q},\omega\right) = \mathbf{1}\left(\varepsilon_h - 1\right) - j\frac{\sigma_a}{\omega\varepsilon_0}\left(\mathbf{1} - \frac{D_a}{j\omega + D_a q^2}\mathbf{qq}\right)$$
$$- j\frac{\sigma_b}{\omega\varepsilon_0}\left(\mathbf{1} - \frac{D_b}{j\omega + D_b q^2}\mathbf{qq}\right) \quad (64)$$

where $\sigma_{a,b}$ and $D_{a,b}$ refer to the relevant quantities for natural or artificial materials for charge species/wire meshes a and b. Using

$$\mathbf{P}\left(\mathbf{q},\omega\right) = \varepsilon_0\overline{\chi}\left(\mathbf{q},\omega\right)\cdot\mathbf{E}\left(\mathbf{q},\omega\right) \quad (65)$$

and considering the longitudinal response ($\mathbf{E}_L = \hat{\mathbf{q}}E_L = \hat{\mathbf{z}}E_z$, and similar for $\mathbf{P}$),

$$P_z\left(q\right) = \left(\varepsilon_0\left(\varepsilon_h - 1\right) + \frac{\sigma_a}{j\omega + D_a q^2} + \frac{\sigma_b}{j\omega + D_b q^2}\right)E_z\left(q\right). \quad (66)$$

Converting to the space domain,

$$\Delta_a\Delta_b P_z\left(z\right) = \left(\varepsilon_0\left(\varepsilon_h - 1\right)\Delta_a\Delta_b + \sigma_a\Delta_b + \sigma_b\Delta_a\right)E_z\left(z\right) \quad (67)$$

where E_z is the total (incident, E_z^{inc}, plus scattered, E_z^{scat}) field and where $\Delta_{a,b}$ are second-order differential operators,

$$\Delta_{a,b} = \left(j\omega - D_{a,b}\frac{\partial^2}{\partial z^2}\right). \quad (68)$$

The one-dimensional Green's function is

$$g\left(z,z'\right) = \frac{e^{-jk_0|z-z'|}}{2jk_0} \quad (69)$$

and the scattered field due to current J is [38]

$$E_z^{\mathrm{scat}}\left(z\right) = \frac{1}{j\omega\varepsilon_0}\left(k_0^2 + \frac{d^2}{dz^2}\right)\int_{-L}^{L}\frac{e^{-jk_0|z-z'|}}{2jk_0}J(z')dz'. \quad (70)$$

Using Leibnitz's theorem [39], if $z \in (-L, L)$ then

$$\left(k_0^2 + \frac{d^2}{dz^2}\right)\int_{-L}^{L}\frac{e^{-jk_0|z-z'|}}{2jk_0}J(z')dz' = -J\left(z\right) \quad (71)$$

such that

$$E_z^{\mathrm{scat}}\left(z\right) = -\frac{J\left(z\right)}{j\omega\varepsilon_0} = -\frac{P_z\left(z\right)}{\varepsilon_0} \quad (72)$$

(and the same thing happens in the static case for $g(z,z') = -|z - z'|/2$.) Note also that for $z \notin (-L, L)$

$$\left(k_0^2 + \frac{d^2}{dz^2}\right)\int_{-L}^{L}\frac{e^{-jk_0(z-z')}}{2jk_0}J(z')dz' = 0 \quad (73)$$

and so the slab does not scatter a field. This can also be seen simply by noting that for a longitudinal field $\mathbf{H} = \mathbf{0}$ and $\nabla \times \mathbf{E} = \mathbf{0}$. Hence, Maxwell's equations can be satisfied only if

$j\omega\mathbf{D} + \mathbf{J}^{\mathrm{ext}} = 0$. Thus in the air region $j\omega\varepsilon_0 E_z^{\mathrm{inc}} = -J^{\mathrm{ext}}$ (the field is nonzero only in the regions where one places the distributed source). On the other hand, in the WM we have $j\omega\left(\varepsilon_0 E_z + P_z\right) + J^{\mathrm{ext}} = 0$, or equivalently $j\omega\left(\varepsilon_0 E_z + P_z\right) - j\omega\varepsilon_0 E_z^{\mathrm{inc}} = 0$, which yields $E_z = -P_z/\varepsilon_0 + E_z^{\mathrm{inc}}$.

Inserting $E_z = \left(-P_z/\varepsilon_0 + E_z^{\mathrm{inc}}\right)$ into (67), the differential equation for polarization becomes

$$\left(\alpha_1 - \alpha_2\frac{\partial^2}{\partial z^2} + \alpha_3\frac{\partial^4}{\partial z^4}\right)P_z\left(z\right)$$
$$= \left(\alpha_1^r - \alpha_2^r\frac{\partial^2}{\partial z^2} + \alpha_3^r\frac{\partial^4}{\partial z^4}\right)\varepsilon_0 E_z^{\mathrm{inc}} \quad (74)$$

where

$$\alpha_1 = j\omega\left(\varepsilon_h + \frac{\sigma_a + \sigma_b}{j\omega\varepsilon_0}\right) \quad (75)$$

$$\alpha_2 = \left(D_a + D_b\right)\varepsilon_h + \frac{\sigma_a D_b + \sigma_b D_a}{j\omega\varepsilon_0} \quad (76)$$

$$\alpha_3 = \frac{D_a D_b \varepsilon_h}{j\omega}, \quad (77)$$

and where $\alpha_{1,2,3}^r = \alpha_{1,2,3}$ with ε_h replaced by $\varepsilon_h - 1$. Since E_z^{inc} is constant in space, we arrive at

$$\left(\alpha_1 - \alpha_2\frac{\partial^2}{\partial z^2} + \alpha_3\frac{\partial^4}{\partial z^4}\right)P_z\left(z\right) = \alpha_1^r\varepsilon_0 E_z^{\mathrm{inc}}. \quad (78)$$

In this case we need two additional boundary conditions (one for each charge species/wire mesh network).

At this point we will finish the example assuming the special case of a single charge species/single wire mesh (setting $\sigma_b = D_b = 0$, $\sigma_a = \sigma$, $D_a = D$), such that

$$\left(1 - \frac{1}{k_D^2}\frac{\partial^2}{\partial z^2}\right)P_z = \left(1 - \frac{j\omega}{\varepsilon_h\left(j\omega + \frac{\sigma}{\varepsilon_0\varepsilon_h}\right)}\right)\varepsilon_0 E_z^{\mathrm{inc}} \quad (79)$$

where k_D is the Debye wavenumber,

$$k_D^2 = \frac{j\omega\varepsilon_0\varepsilon_h + \sigma}{D\varepsilon_0\varepsilon_h}. \quad (80)$$

Note that if $D = 0$ spatial dispersion is absent and the solution of (79) (after rearranging to accommodate $D = 0$) is constant inside the slab,

$$P_z = \frac{j\omega\varepsilon_0\left(\varepsilon_h - 1\right) + \sigma}{j\omega\varepsilon_0\varepsilon_h + \sigma}\varepsilon_0 E_z^{\mathrm{inc}}. \quad (81)$$

For $D \to \infty$,

$$\frac{\partial^2}{\partial z^2}P_z = \frac{\left(j\omega\varepsilon_0\left(\varepsilon_h - 1\right) + \sigma\right)}{-\varepsilon_h D}E_z^{\mathrm{inc}} = 0 \to P_z = C_1 z + C_2. \quad (82)$$

Enforcing $P(-L) = P(L)$ by symmetry, $P_z = C_2$, and enforcing the ABC $\varepsilon_0 E_z^{\mathrm{inc}} = \varepsilon_h\varepsilon_0\left(E_z^{\mathrm{inc}} + E_z^{\mathrm{scat}}\right)$ leads to

$$P_z = \left(1 - \frac{1}{\varepsilon_h}\right)\varepsilon_0 E_z^{\mathrm{inc}} \quad (83)$$

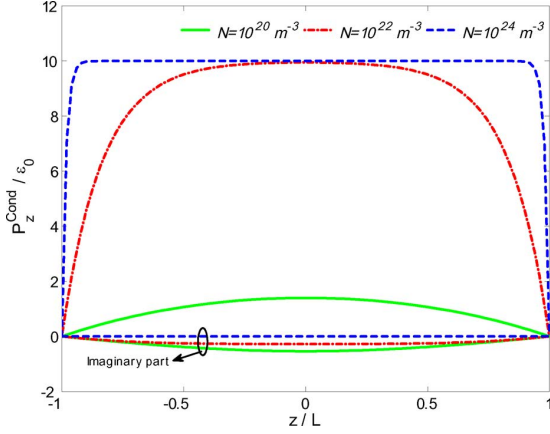which is also the $D = 0$ result if $\sigma \to 0$.

Fig. 5. Conductive part of the polarization for a semiconductor with $E^{\text{inc}} = 10$ V/m, $f = 10$ GHz, $L = 250$ nm, $T = 300$ K, $\tau = 2.16 \times 10^{-13}$ s, $\varepsilon_h = 11.9$, and $m_{eff} = 0.26 m_e$, for charge (doping) number density $N = 10^{20}, 10^{22}$, and 10^{24} m^{-3}. Higher doping leads to better screening.

For D finite and not zero, the solution of (79) is even in z and is given by

$$P_z = C \cosh (k_D z) + \left(1 - \frac{j\omega}{\varepsilon_h \left(j\omega + \frac{\sigma}{\varepsilon_0 \varepsilon_h} \right)} \right) \varepsilon_0 E_z^{\text{inc}} \quad (84)$$

and enforcing the ABC $\varepsilon_0 E_z^{\text{inc}} = \varepsilon_h \varepsilon_0 \left(E_z^{\text{inc}} + E_z^{\text{scat}} \right)$ leads to

$$P_z(z) = \left(\frac{j\omega}{\varepsilon_h \left(j\omega + \frac{\sigma}{\varepsilon_0 \varepsilon_h} \right)} - \frac{1}{\varepsilon_h} \right) \varepsilon_0 E_z^{\text{inc}} \frac{\cosh (k_D z)}{\cosh (k_D L)}$$

$$+ \left(1 - \frac{j\omega}{\varepsilon_h \left(j\omega + \frac{\sigma}{\varepsilon_0 \varepsilon_h} \right)} \right) \varepsilon_0 E_z^{\text{inc}}. \quad (85)$$

In the following we show the conductive part of the polarization

$$\frac{P_z^{\text{cond}}(z)}{\varepsilon_0} = \frac{P_z(z)}{\varepsilon_0} - (\varepsilon_h - 1) E_z^{\text{total}}(z)$$

$$= \frac{P_z(z)}{\varepsilon_0} - (\varepsilon_h - 1) \left(-\frac{P_z(z)}{\varepsilon_0} + E^{\text{inc}} \right) \quad (86)$$

for several different materials, with $E^{\text{inc}} = 10$ V/m. Fig. 5 shows the response in a semiconducting material slab at $f = 10$ GHz, for $L = 250$ nm, $T = 300$ K, $\tau = 2.16 \times 10^{-13}$ s, $\varepsilon_h = 11.9$, and $m_{eff} = 0.26 m_e$, for charge (doping) number density $N = 10^{20}, 10^{22}$, and 10^{24} m^{-3}.

It can be seen that as doping increases, the response is less affected by diffusion (conduction dominates), and the response becomes more metal-like, as expected. Considering the values in Table I, even though the diffusion coefficient is independent of doping, as doping increases conduction increases, the Debye wavenumber increases, and the Debye length decreases, such that screening becomes more effective. Fig. 6 shows the same structure, but for fixed $N = 10^{22}$ m^{-3}, at several different temperatures. In this case, since $D \propto T$ (we assume that σ is independent of temperature, i.e., that the free electron density
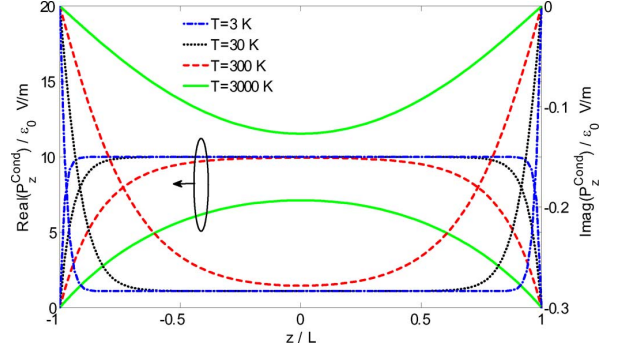

Fig. 6. Conductive part of the polarization for a semiconductor with $E^{\text{inc}} = 10$ V/m, $f = 10$ GHz, $L = 250$ nm, $\tau = 2.16 \times 10^{-13}$ s, $\varepsilon_h = 11.9$, and $m_{eff} = 0.26 m_e$, for charge (doping) number density $N = 10^{22}$ m^{-3} at several different temperatures. Higher temperature leads to more diffusion.

is N at all temperatures), we see that diffusion becomes more effective at higher temperatures, as expected.

Fig. 7(a) shows the same semiconductor structure at $f = 5$ THz, for two doping densities in the vicinity of $N = 10^{23}$. These correspond to frequencies below ($N = 5 \times 10^{23}$ m^{-3}, $f_p = 3.61$ THz) and above ($N = 15 \times 10^{23}$ m^{-3}, $f_p = 6.25$ THz) the plasma frequency $f_p = \sqrt{N q^2/m_{eff}\varepsilon}/2\pi$. There are subwavelength ripples in the field for frequencies near to, and on both sides of the plasma frequency (also observed for metals near the plasma frequency [3]), but sufficiently far above the plasma frequency the field is smooth (not shown). Fig. 7(b) shows the total field both inside and outside the slab for the same two frequencies as in Fig. 7(a), and Fig. 7(c) shows the same quantities as Fig. 7(a), except for $T = 30$ K (i.e., multiplying the diffusion coefficient by 0.1). It can be seen that diminished diffusion results in better field screening, as expected. In the limit that $D \to 0$, the field is constant inside the slab, given by (81).

Fig. 8 shows the response of a connected isotropic wire medium made from PEC wires, $\varepsilon_h = 1$, $f = 10$ GHz , wire period $a = \lambda_0/100$, $\lambda_0/10$, and $\lambda_0/5$, wire radius $r = a/100$, and slab width $L = \lambda_0/4 = 7.49$ mm. It can be seen that as the wire period becomes larger, diffusion becomes more important (since σ decreases strongly with increasing period). However, far-subwavelength ripples similar to those shown in Fig. 7(a)–(c) are not induced for the PEC wire medium since the Debye wave number k_D is purely real, as can be seen from (27) and (36) and from Tables I–II. From (79) it is seen that this implies that P_z depends on z as a damped exponential, and to have ripples one needs k_D to be complex valued, which happens for semiconductors and other natural materials, but not for PEC wire media.

VI. ISOTROPIC CONNECTED DOUBLE WIRE MESH EXAMPLE

To further illustrate the richness of the physics of spatially dispersive media, next we extend the analysis of the previous section, and consider the scattering of a (transverse) plane wave by a semi-infinite half space filled with the connected double wire mesh (metamaterial of Fig. 2). Comparing (19) and (39), it is evident that with an appropriate definition of variables, the following is also valid for a two-component plasma.
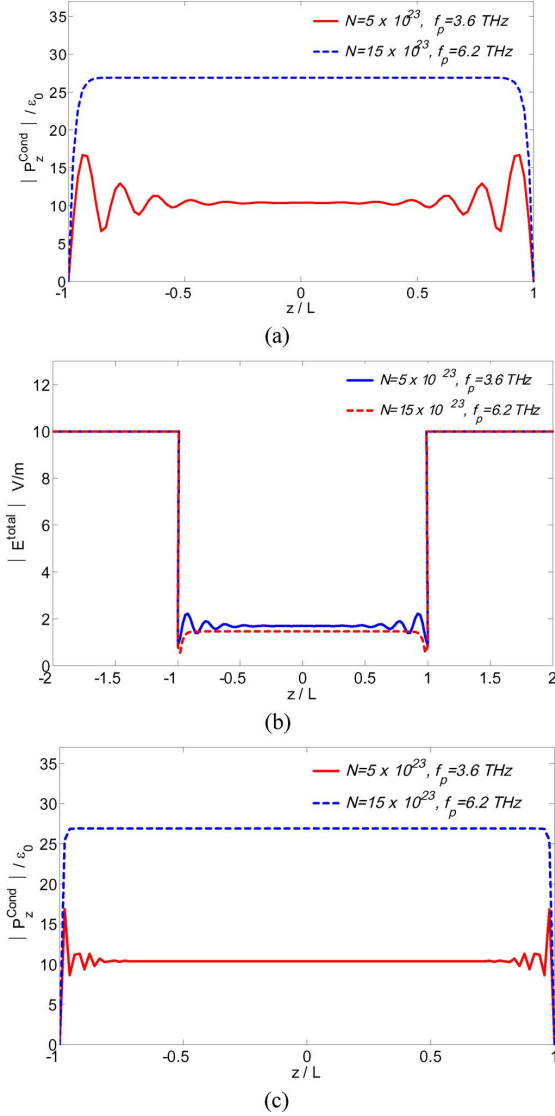
(a)

(b)

(c)

Fig. 7. (a) Conductive part of the polarization for a semiconductor with $E^{\text{inc}} = 10$ V/m, $f = 5$ THz, $L = 250$ nm, $T = 300$ K, $\tau = 2.16 \times 10^{-13}$ s, $\varepsilon_h = 11.9$, and $m_{eff} = 0.26 m_e$, for charge (doping) number density $N = 5 \times 10^{23}$ and 15×10^{23} m^{-3}. (b) Total electric field outside and inside the slab for the same two frequencies as in Fig. 6(a). (c) Same as (a) except $T = 30$ K. Diffusion is reduced and screening is more effective than at $T = 300$ K.

A. Plane Wave Modes

To begin with, we characterize the plane wave solutions supported by the unbounded effective medium. Equation (40) implies that the plane wave normal modes can be classified as transverse modes (with polarization perpendicular to the wavevector **q**), and longitudinal modes (with polarization parallel to the wavevector **q**). The effective permittivity seen by the transverse modes is $\varepsilon_t(\omega)$, whereas the permittivity seen by the longitudinal modes is $\varepsilon_l(\omega, q)$. Thus, the dispersion characteristic of the transverse modes is given by,

$$q^2 = \varepsilon_t(\omega) \frac{\omega^2}{c^2} \quad \text{(transverse modes)} \quad (87)$$

whereas the dispersion equation of the longitudinal modes is

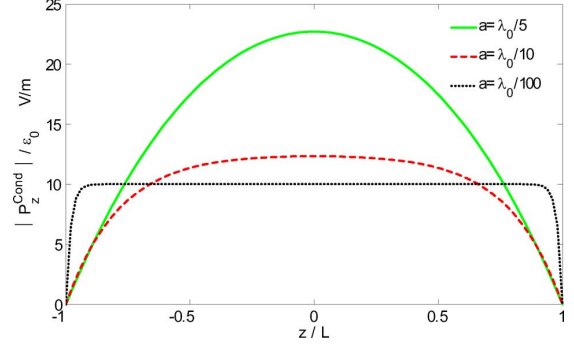$$\varepsilon_l(\omega, q) = 0 \quad \text{(longitudinal modes)}. \quad (88)$$

Fig. 8. Conductive part of the polarization for a PEC connected isotropic wire medium, having $\varepsilon_h = 1$, $f = 10$ GHz, $r = a/100$, $L = \lambda_0/4 = 7.49$ mm for several different wire periods, $a = \lambda_0/100$, $\lambda_0/10$, and $\lambda_0/5$. As the wire period becomes larger, diffusion becomes more important.

Solving the dispersion characteristic of the longitudinal modes with respect to q it is found that

$$q^2 = \frac{1}{2} \left\{ -k_{pA}^2 l_{0A} - k_{pB}^2 l_{0B} + \frac{\omega^2}{c^2}(l_{0A} + l_{0B}) \right.$$
$$\pm \left[4\left(k_{pA}^2 + k_{pB}^2 - \frac{\omega^2}{c^2}\right)\frac{\omega^2}{c^2} l_{0A} l_{0B} \right.$$
$$\left. \left(-k_{pA}^2 l_{0A} - k_{pB}^2 l_{0B} + \frac{\omega^2}{c^2}(l_{0A}+l_{0B})\right)^2 \right]^{1/2} \left. \right\}. \quad (89)$$

It is manifest from the above result that the effective medium supports *two* distinct longitudinal modes, with different propagation constants. This is rather unusual since both natural one-component plasmas and connected isotropic wire media with a single metallic network (Fig. 1) typically support a single longitudinal mode [20], [29], [40]. Even more curious, it can be checked that in the limit $l_{0A}, l_{0B} \to l_0$ and $k_{pA}, k_{pB} \to k_p$, so that the two networks become identical, the two longitudinal modes have the dispersions

$$q^2 = l_0 \frac{\omega^2}{c^2} - l_0 k_{p,eff}^2; \quad q^2 = l_0 \frac{\omega^2}{c^2}. \quad (90)$$

Thus, in this situation, one of the longitudinal modes has no cut-off, and can propagate at arbitrarily low frequencies! This is quite odd, but it is actually consistent with the photonic band structure calculations reported in Fig. 1 of [23]. Hence, our effective medium model seems to reproduce some of the key features of the photonic band structure of the material. The reason for the emergence of a propagating longitudinal mode is clearly related to the fact that the metamaterial is formed by two *non-connected* metallic networks, which may be set at different electric potentials.

B. The Reflection Problem

Suppose now that a transverse plane wave propagating in free space ($z < 0$) impinges on a semi-infinite block of the connected double wire mesh ($z > 0$). The incoming magnetic field is along the x-direction, and the direction of propagation is in the yoz plane, so that the incident wave is transverse magnetic (TM)-polarized (inset of Fig. 8). Evidently, an incident

wave may in general excite both the transverse and longitudinal modes supported by the wire medium. For the geometry under study three modes can be excited: two longitudinal modes and a TM-polarized transverse mode (the wire medium supports an additional mode with transverse electric (TE) polarization, which is not coupled to the incident field).

Taking into account that the macroscopic magnetic field associated with the longitudinal modes vanishes, and supposing that the amplitude of the incoming magnetic field is normalized to unity, it follows that the magnetic field in all space is of the form (the y-variation of the field is suppressed)

$$H_x = e^{-\gamma_0 z} + R e^{\gamma_0 z}, \quad z < 0$$
$$H_x = A_T e^{-j q_z^{(T)} z}, \quad z > 0 \tag{91}$$

where R is the reflection coefficient, $\gamma_0 = \sqrt{q_y^2 - (\omega/c)^2}$ ($q_y = (\omega/c) \sin\theta_i$ for a propagating incoming plane wave that illuminates the interface along the direction θ_i), $q_z^{(T)}$ is the propagation constant along z of the transverse mode in the wire medium, and A_T is an unknown constant. From (87), we can write that $j q_z^{(T)} = \sqrt{q_y^2 - \varepsilon_t \omega^2/c^2}$.

On the other hand, the electric field depends not only on the transverse fields but also on the longitudinal fields in the wire medium. Since for transverse plane waves we can write $\mathbf{E} = \hat{\mathbf{x}} \times \mathbf{q} \, H_x/(\omega\varepsilon)$, it follows that

$$\mathbf{E} = \frac{1}{\omega\varepsilon_0} \left(\hat{\mathbf{x}} \times \mathbf{q}_0^+ e^{-\gamma_0 z} + \hat{\mathbf{x}} \times \mathbf{q}_0^- R e^{\gamma_0 z} \right), \quad z < 0$$
$$\mathbf{E} = \frac{1}{\omega\varepsilon_0} \left(B_1 \mathbf{q}_{L,1}^+ e^{-j q_z^{(L,1)} z} + B_2 \mathbf{q}_{L,2}^+ e^{-j q_z^{(L,2)} z} \right)$$
$$+ \frac{1}{\omega\varepsilon_0\varepsilon_t(\omega)} \hat{\mathbf{x}} \times \mathbf{q}_T^+ A_T e^{-j q_z^{(T)} z}, \quad z > 0. \tag{92}$$

In the above, $\mathbf{q}_0^{\pm} = (0, q_y, -(\pm j\gamma_0))$ is the wavevector in free-space, $\mathbf{q}_T^+ = \left(0, q_y, q_z^{(T)}\right)$ and $\mathbf{q}_{L,i}^+ = \left(0, q_y, q_z^{(L,i)}\right)$, $i = 1, 2$, are the wave vectors associated with the transverse and longitudinal modes in the artificial plasma, respectively. The constants B_1 and B_2 represent the unknown complex amplitudes of the longitudinal modes in the wire medium. The wave number $q_z^{(L,i)}$ is determined by noting that $\mathbf{q}_{L,i}^+$ is a solution of the dispersion (89).

C. Additional Boundary Conditions

To determine the unknown coefficients, we need to impose boundary conditions at the interface $z = 0$. The continuity of the magnetic field and of the tangential (y-component) of the electric field yield

$$1 + R = A_T$$
$$j\gamma_0 (1 - R) = \frac{-q_z^{(T)} A_T}{\varepsilon_t} + (B_1 + B_2) q_y. \tag{93}$$

Clearly, since we have two extra modes (the longitudinal waves) two additional boundary conditions are required to determine all the unknowns. This is understandable from the discussion of Section IV: since here we have two independent networks (which is the metamaterial analogue of a natural material in which the conduction properties are determined by two carrier

species) it is necessary that the z-component of the conduction current transported by each individual network vanishes at the interface. Since we assume that $\varepsilon_h = 1$, it is obvious that this can be guaranteed simply by

$$\mathbf{P}_A^{\mathrm{cond}} \cdot \hat{\mathbf{z}} = 0, \quad \mathbf{P}_B^{\mathrm{cond}} \cdot \hat{\mathbf{z}} = 0 \tag{94}$$

where $\mathbf{P}_A^{\mathrm{cond}}$ is the contribution from mesh A to the conductive polarization of the effective medium and $\mathbf{P}_B^{\mathrm{cond}}$ is defined in the same manner.

Using the fact that for each eigenmode $\mathbf{P}_A^{\mathrm{cond}} = \left(\overline{\boldsymbol{\varepsilon}}^A - \varepsilon_0 \mathbf{1}\right) \cdot \mathbf{E}$, i.e.,

$$\frac{\mathbf{P}_A^{\mathrm{cond}}}{\varepsilon_0} = \left[(\varepsilon_{tA} - 1)\left(\mathbf{1} - \frac{\mathbf{q}\mathbf{q}}{q^2} \right) + (\varepsilon_{lA}(q) - 1) \frac{\mathbf{q}\mathbf{q}}{q^2} \right] \cdot \mathbf{E} \tag{95}$$

with $\varepsilon_{tA} = 1 - k_{pA}^2/(\omega^2/c^2)$ and $\varepsilon_{lA} = 1 + k_{pA}^2/(q^2/l_{0A} - \omega^2/c^2)$, and that the total field in the wire medium is a superposition of three modes, it follows from $\mathbf{P}_A^{\mathrm{cond}} \cdot \hat{\mathbf{z}} = 0$ that

$$\hat{\mathbf{z}} \cdot \Bigg[B_1 (\varepsilon_{lA,1} - 1) \mathbf{q}_{L,1}^+ + B_2 (\varepsilon_{lA,2} - 1) \mathbf{q}_{L,2}^+$$
$$+ \frac{\varepsilon_{tA} - 1}{\varepsilon_t} \hat{\mathbf{x}} \times \mathbf{q}_T^+ A_T \Bigg] = 0 \tag{96}$$

with $\varepsilon_{lA,i} = \varepsilon_{lA,i}\left(\mathbf{q}_{L,i}^+\right)$. This ABC is equivalent to

$$B_1(\varepsilon_{lA,1} - 1) q_z^{(L,1)} + B_2 (\varepsilon_{lA,2} - 1) q_z^{(L,2)} + \frac{\varepsilon_{tA} - 1}{\varepsilon_t} q_y A_T = 0. \tag{97}$$

Obviously, it is possible to write a similar equation for the network B,

$$B_1(\varepsilon_{lB,1} - 1) q_z^{(L,1)} + B_2 (\varepsilon_{lB,2} - 1) q_z^{(L,2)} + \frac{\varepsilon_{tB} - 1}{\varepsilon_t} q_y A_T = 0 \tag{98}$$

where we put $\varepsilon_{tB} = 1 - k_{pB}^2/(\omega^2/c^2)$, $\varepsilon_{lB} = 1 + k_{pB}^2/(q^2/l_{0B} - \omega^2/c^2)$, and $\varepsilon_{lB,i} = \varepsilon_{lB,i}\left(\mathbf{q}_{L,i}^+\right)$. Equations (97) and (98) arise from the two required additional boundary conditions. By solving the linear system defined by (93), (97) and (98), it is possible to determine all the unknowns and obtain the solution of the scattering problem.

D. Numerical Example and Discussion

The fact that the connected double wire mesh supports a propagating mode for arbitrarily low frequencies, suggests that it may be possible to couple energy from the free-space region into the metamaterial, even if the frequency is below the effective plasma frequency. To assess such a counterintuitive possibility, we numerically solved the linear system formulated in the previous subsection for the case of a metamaterial such that the radii of the two networks is $r_A = 0.001a$ and $r_B = 0.05a$. The computed fractional reflected power (reflectivity), $|R|^2$, is depicted in Fig. 9 as a function of frequency for different angles of incidence. As seen, for frequencies below the effective plasma frequency ($k_{p,eff} = 2.2/a$) the wave is nearly perfectly reflected. However, within our homogenization model, the transmission into the artificial plasma, even if tiny, is not
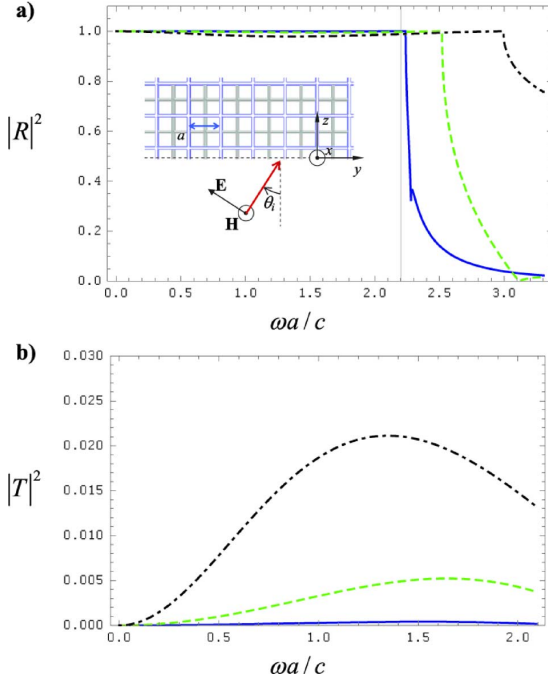
Fig. 9. (a) Reflectivity ($|R|^2$) as a function of the normalized frequency for: (i) $\theta_i = 15°$ (solid blue line), (ii) $\theta_i = 45°$ (dashed green line) and (iii) $\theta_i = 80°$ (dot-dashed black line). The dashed vertical line represents the effective plasma wave number $k_{p,eff}$. (b) Similar to (a) but for the transmissivity ($|T|^2 = 1 - |R|^2$). The inset in (a) shows the geometry of the problem.

exactly zero due to a residual excitation of the propagating longitudinal mode. Indeed, panel (b) of Fig. 9 shows that the fractional transmitted power (transmissivity) can surpass 2% for frequencies well below the effective plasma frequency. The level of transmission is stronger for wide incident angles (the maximum of transmission typically occurs close to $\theta_i = 80°$). Indeed, it is well known that for normal incidence the longitudinal modes cannot be excited. To conclude, we point out that a non-zero transmission into the metamaterial is only possible if the two networks are different ($r_A \neq r_B$). It can be shown that if the two metallic networks are identical the propagating longitudinal mode is impossible to excite with a macroscopic external excitation.

VII. CONCLUSIONS

In this work, we have shown that similar to semiconductors and metals, the nonlocal response of wire media can be understood in terms of a drift-diffusion transport model. We have highlighted the many similarities and the differences between spatially dispersive natural media and artificial wire media, and we have introduced an effective Debye wavenumber/length as a quantitative measure of spatial dispersion. It was shown that for several geometries Pekar's ABC can describe the response of wire media, but, very importantly, it must be enforced only on the conductive component of the total polarization induced in the wire medium. We have presented a simple one-dimensional example with closed-form solution that highlights these topics. Finally, we have proposed a novel effective medium model to describe the double isotropic wire medium, and illustrated how this model can be instrumental in the solution of a scattering problem.

APPENDIX
SCATTERING/RESONATOR PROBLEMS BASED ON THE TRANSPORT MODEL FOR WIRE MEDIA

It was shown in the paper that the transport equation for mobile charges in a natural material, with a local polarization model, leads to an effective permittivity tensor (17) that has the same form as that obtained for a variety of artificial wire materials. Therefore, the transport/drift-diffusion model can be used to model artificial wire materials in various applications, such as for scattering or resonator problems. The general transport-based scattering/resonator problem is based on (13) and (16) using the self-consistent field $\mathbf{E}$ due to both polarization and conduction currents, and applying the necessary additional boundary conditions. For an isotropic wire-medium scatterer having volume Ω immersed in a homogeneous background having permittivity ε_1, the coupled equations to be solved are

$$\mathbf{J}^{\text{pol}}(\mathbf{r}) - (j\omega[\varepsilon - \varepsilon_1])\mathbf{E}^{\text{inc}}(\mathbf{r})$$
$$= \frac{\varepsilon - \varepsilon_1}{\varepsilon_1}\left(k_1^2 + \nabla\nabla\cdot\right)\int_\Omega g(\mathbf{r},\mathbf{r}')\left(\mathbf{J}^{\text{pol}}(\mathbf{r}') + \mathbf{J}^{\text{cond}}(\mathbf{r}')\right)d\Omega'$$
$$(99)$$

$$\left(1 - \frac{D(\omega)}{j\omega}\nabla\nabla\cdot\right)\mathbf{J}^{\text{cond}}(\mathbf{r}) - \sigma(\omega)\mathbf{E}^{\text{inc}}(\mathbf{r})$$
$$= \frac{\sigma(\omega)}{j\omega\varepsilon_1}\left(k_1^2 + \nabla\nabla\cdot\right)\int_\Omega g(\mathbf{r},\mathbf{r}')\left(\mathbf{J}^{\text{pol}}(\mathbf{r}') + \mathbf{J}^{\text{cond}}(\mathbf{r}')\right)d\Omega'$$
$$(100)$$

for $\mathbf{r} \in \Omega$, where k_1 is the wavenumber in the background environment and $g(\mathbf{r},\mathbf{r}') = e^{-jk_1R}/4\pi R$, where $R = |\mathbf{r} - \mathbf{r}'|$. For a resonator problem natural modes are obtained from $\mathbf{E}^{\text{inc}} = \mathbf{0}$, and for a uniaxial wire medium (99) become simplified somewhat. The formulation (99)-(100) is very attractive compared to a real-space convolution form $\mathbf{J}(\mathbf{r}) = \int_\Omega \overline{\boldsymbol{\sigma}}(\mathbf{r} - \mathbf{r}',\omega) \cdot \mathbf{E}(\mathbf{r}')d\Omega'$ since in that case one obtains a six-fold integral equation (three associated with the convolution and three associated with relating the electric field to current), whereas in the transport model one obtains a three-dimensional integral equation. General two- and three-dimensional wire medium scattering problems based on (99)-(100) will be reported in a separate work.

REFERENCES

[1] L. D. Landau, E. M. Lifshitz, and L. P. Pitaevskii, *Electrodynamics of Continuous Media*, 2nd ed. Amsterdam: Elsevier, 1984.
[2] *Spatial Dispersion in Solids and Plasmas*, P. Halevi, Ed. Amsterdam: North Holland, 1992.
[3] F. Forstmann and R. R. Gerhardts, *Metal Optics Near the Plasma Frequency*. Heidelberg: Springer Berlin, 1982.
[4] M. Dressel and G. Grüner, *Electrodynamics of Solids*. Cambridge: Cambridge University Press, 2002.
[5] P. A. Belov, R. Marqués, S. I. Maslovski, I. S. Nefedov, M. Silveirinha, C. R. Simovski, and S. A. Tretyakov, "Strong spatial dispersion in wire media in the very large wavelength limit," *Phys. Rev. B*, vol. 67, pp. 113103 (1)–(4), 2003.
[6] P. Burghignoli, G. Lovat, F. Capolino, D. R. Jackson, and D. R. Wilton, "Directive leaky-wave radiation from a dipole source in a wire-medium slab," *IEEE Trans. Antennas. Propag.*, vol. 56, pp. 1329–1338, 2008.
[7] A. Demetriadou and J. B. Pendry, "Taming spatial dispersion in wire metamaterial," *J. Phys.: Condens. Matter*, vol. 20, pp. 295222 (1)–(11), 2008.

[8] A. B. Yakovlev, M. G. Silveirinha, O. Luukkonen, C. R. Simovski, I. S. Nefedov, and S. A. Tretyakov, "Characterization of surface-wave and leaky-wave propagation on wire-medium slabs and mushroom structures based on local and nonlocal homogenization models," *IEEE Trans. Microw. Theory Tech.*, vol. 57, pp. 2700–2714, 2009.

[9] P. A. Belov and M. Silveirinha, "Resolution of subwavelength transmission devices formed by a wire medium," *Phys. Rev. E*, vol. 73, pp. 056607 (1)–(9), 2006.

[10] X. Radu, D. Garray, and C. Craeye, "Toward a wire medium endoscope for MRI imaging," *Metamaterials*, vol. 3, pp. 90–99, Oct. 2009.

[11] P. A. Belov, G. K. Palikaras, Y. Zhao, A. Rahman, C. R. Simovski, Y. Hao, and C. Parini, "Experimental demonstration of multiwire endoscopes capable of manipulating near-fields with subwavelength resolution," *Appl. Phys. Lett.*, vol. 97, pp. 191905 (1)–(3), 2010.

[12] T. A. Morgado, J. S. Marcos, M. G. Silveirinha, and S. I. Maslovski, "Experimental verification of full reconstruction of the near-field with a metamaterial lens," *Appl. Phys. Lett.*, vol. 97, pp. 144102 (1)–(3), 2010.

[13] P. Burghignoli, G. Lovat, F. Capolino, D. R. Jackson, and D. R. Wilton, "Highly polarized, directive radiation from a Fabry-Pérot cavity leaky-wave antenna based on a metal strip grating," *IEEE Trans. Antennas Propag.*, vol. 58, pp. 3873–3883, Dec. 2010.

[14] S. Paulotto, P. Baccarelli, P. Burghignoli, G. Lovat, G. W. Hanson, and A. B. Yakovlev, "Homogenized Green's Functions for an aperiodic line source over planar densely-periodic artificial impedance surfaces," *IEEE Trans. Microwave Theory Tech.*, vol. 58, pp. 1807–1817, Jul. 2010.

[15] G. W. Hanson, "Drift-diffusion: A model for teaching spatial dispersion concepts and the importance of screening in nanoscale structures," *IEEE Antennas Propag. Mag.*, vol. 52, pp. 198–207, Oct. 2010.

[16] J. A. Bittencourt, *Fundamentals of Plasma Physics*, 3rd ed. New York: Springer-Verlag.

[17] B. B. Dasgupta and R. Fuchs, "Polarizability of a small sphere including nonlocal effects," *Phys. Rev. B*, vol. 24, pp. 554–561, 1981.

[18] R. Ruppin, "Optical properties of spatially dispersive dielectric spheres," *J. Opt. Soc. Am.*, vol. 71, pp. 755–758, 1981.

[19] A. M. Portis, *Electromagnetic Fields: Sources and Media*. New York: Wiley, 1978.

[20] M. G. Silveirinha, "Artificial plasma formed by connected metallic wires at infrared frequencies," *Phys. Rev. B*, vol. 79, pp. 035118 (1)–(15), 2009.

[21] M. G. Silveirinha and C. A. Fernandes, "Homogenization of 3-D-connected and nonconnected wire metamaterials," *IEEE Trans. Microw. Theory Tech.*, vol. 53, pp. 1418–1430, 2005.

[22] S. I. Maslovski and M. G. Silveirinha, "Nonlocal permittivity from a quasistatic model for a class of wire media," *Phys. Rev B*, vol. 80, pp. 245101 (1)–(10), 2009.

[23] J. Shin, J.-T. Shen, and S. Fan, "Three-dimensional electromagnetic metamaterials that homogenize to uniform non-Maxwellian media," *Phys. Rev B*, vol. 76, pp. 113101 (1)–(4), 2007.

[24] M. G. Silveirinha, "Nonlocal homogenization theory of structured materials," in *Theory and Phenomena of Artificial Materials*, F. Capolino, Ed. Boca Raton: CRC Press, 2009, vol. 1.

[25] I. Nefedov and S. Tretyakov, "Ultrabroadband electromagnetically indefinite medium formed by aligned carbon nanotubes," *Phys. Rev B*, vol. 84, pp. 113410 (1)–(4), 2011.

[26] S. I. Pekar, *Zh. Eksp. Teor Fiz*, vol. 33, p. 1022, 1957.

[27] W. A. Davis and C. M. Krowne, "The effects of drift and diffusion in semiconductors on plane wave interaction at interfaces," *IEEE Trans. Antennas. Propag.*, vol. 36, pp. 97–103, 1988.

[28] A. D. Boardman and R. Ruppin, "The boundary conditions between spatially dispersive media," *Surface Sci.*, vol. 112, pp. 153–167, 1981.

[29] A. R. Melnyk and M. J. Harrison, "Theory of optical excitation of plasmons in metals," *Phys. Rev. B*, vol. 2, pp. 835–850, 1970.

[30] M. Anderegg, B. Feuerbacher, and B. Fitton, "Optically excited longitudinal plasmons in Potassium," *Phys. Rev. Lett.*, vol. 27, p. 1565, 1971.

[31] M. Silveirinha, "Additional boundary conditions for the wire medium," *IEEE Trans. Antennas. Propag.*, vol. 54, pp. 1766–1780, 2006.

[32] M. G. Silveirinha, "Additional boundary conditions for nonconnected wire media," *New J. Phys.*, vol. 11, pp. 113016 (1)–(27), 2009.

[33] O. Luukkonen, M. Silveirinha, A. Yakovlev, C. Simovski, I. Nefedov, and S. Tretyakov, "Effects of spatial dispersion on reflection from mushroom-type artificial impedance surfaces," *IEEE Trans. Microw. Theory Tech.*, vol. 57, pp. 2692–2699, 2009.

[34] A. B. Yakovlev, Y. R. Padooru, S. Karbasi, G. W. Hanson, and A. Mafi, "Nonlocal homogenization model for the analysis of absorbing properties of mushroom structures with graphene patches at microwaves," presented at the IEEE AP-S Int. Symp. and URSI Radio Science Meeting, Toronto, ON, Canada, Jul. 11–17, 2010.

[35] M. Silveirinha, C. A. Fernandes, and J. R. Costa, "Additional boundary condition for a wire medium connected to a metallic surface," *New J. Phys.*, vol. 10, p. 053011, 2008.

[36] A. B. Yakovlev, Y. R. Padooru, G. W. Hanson, A. Mafi, and S. Karbasi, "A generalized additional boundary condition for mushroom-type and bed-of-nails-type wire media," *IEEE Trans. Microw. Theory Tech.*, vol. 59, no. 3, pp. 527–532, Mar. 2011.

[37] S. I. Maslovski, T. A. Morgado, M. G. Silveirinha, C. S. R. Kaipa, and A. B. Yakovlev, "Generalized additional boundary conditions for wire media," *New J. Phys.*, vol. 12, pp. 113047 (1)–(19), 2010.

[38] A. Ishimaru, *Electromagnetic Wave Propagation, Radiation, and Scattering*. Engelwood Cliffs, NJ: Prentice Hall, 1991.

[39] A. Mattuck, *Introduction to Analysis*. Engelwood Cliffs, NJ: Prentice-Hall, 1999.

[40] N. W. Ashcroft and N. D. Mermin, *Solid State Physics*. Philadelphia, PA: Holt, Rinehart, and Winston, 1975.

George W. Hanson (S'85–M'91–SM'98–F'09) was born in Glen Ridge, NJ, in 1963. He received the B.S.E.E. degree from Lehigh University, Bethlehem, PA, the M.S.E.E. degree from Southern Methodist University, Dallas, TX, and the Ph.D. degree from Michigan State University, East Lansing, in 1986, 1988, and 1991, respectively.

From 1986 to 1988, he was a development Engineer with General Dynamics, Fort Worth, TX, where he worked on radar simulators. From 1988 to 1991, he was a Research and Teaching Assistant in the Department of Electrical Engineering, Michigan State University. He is currently a Professor of electrical engineering and computer science at the University of Wisconsin, Milwaukee. His research interests include nanoelectromagnetics, mathematical methods in electromagnetics, electromagnetic wave phenomena in layered media, integrated transmission lines, waveguides, and antennas, and leaky wave phenomena. He is coauthor of the book *Operator Theory for Electromagnetics: An Introduction* (Springer, New York, 2002) and author of *Fundamentals of Nanoelectronics* (Prentice-Hall, NJ, 2007).

Dr. Hanson is a member of URSI Commission B, Sigma Xi, and Eta Kappa Nu, and was an Associate Editor for the IEEE TRANSACTIONS ON ANTENNAS AND PROPAGATION from 2002–2007. In 2006 he received the S.A. Schelkunoff Best Paper Award from the IEEE Antennas and Propagation Society.

Ebrahim Forati (S'11) was born in Iran in 1983. He received the B.Sc. and M.Sc degrees from Iran University of Science and Technology (IUST), Tehran, in 2006 and 2009, respectively. He is currently working toward the Ph.D. degree at the University of Wisconsin Milwaukee (UWM).

Previously, he was a Research Assistant in the Electromagnetic Engineering Research Laboratory at IUST and is now a teaching assistant at UWM. His current areas of research interests include electromagnetics and metamaterials.

Mário G. Silveirinha (S'99–M'03) received the "Licenciado" degree in electrical engineering from the University of Coimbra, Portugal, in 1998 and the Ph.D. degree in electrical and computer engineering from the Instituto Superior Técnico (IST), Technical University of Lisbon, Portugal, in 2003.

Since 2003, he is an Assistant Professor at the University of Coimbra. His research interests include electromagnetic wave propagation in structured materials and effective medium theory.